diversity

MDPI

Article

Phylogenetic Assessment of Freshwater Mussels *Castalia ambigua* and *C. inflata* at an Ecotone in the Paraguay River Basin, Brazil Shows That Inflated and Compressed Shell Morphotypes Are the Same Species

Miluska Olivera-Hyde [1], Eric Hallerman [1,*], Rogério Santos [2], Jess Jones [1,3], Brianne Varnerin [1,†], Guilherme da Cruz Santos Neto [4], Maria Cristina Mansur [2], Priscilla Moraleco [2] and Claudia Callil [2]

1 Department of Fish and Wildlife Conservation, Virginia Polytechnic Institute and State University, Blacksburg, VA 24061, USA; mohyde@vt.edu (M.O.-H.); jess_jones@fws.gov (J.J.); bvv0002@auburn.edu (B.V.)
2 ECOBIV—Conservation and Ecology of Freshwater Mussel Group, Bioscience Institute of Federal University of Mato Grosso—UFMT, Av. Fernando Correa da Costa 2367, Cuiabá 78060-900, MT, Brazil; roger.c.l.santos@gmail.com (R.S.); mcrismansur@gmail.com (M.C.M.); priscilladm@gmail.com (P.M.); callil@ufmt.br (C.C.)
3 U.S. Fish and Wildlife Service, Blacksburg, VA 24061, USA
4 Laboratory of Molecular Biology and Neuroecology, Federal Institute of Para—Braganza Campus, Av. dos Bragancanos S/N, Bairro Vila Sinha, Braganca CEP 68600-000, PA, Brazil; guilherneto@gmail.com
* Correspondence: ehallerm@vt.edu; Tel.: +1-540-231-3257
† Current address: Department of Biology, Auburn University, Auburn, AL 36849, USA.

Received: 25 October 2020; Accepted: 11 December 2020; Published: 16 December 2020

Abstract: The phylogeny and taxonomy of freshwater mussels of the genus *Castalia* in South America is complicated by issues of morphological plasticity and limited molecular genetic data. We present field data on the distributions of the nominal *Castalia ambigua* and *C. inflata* in the upper Paraguay River basin in Brazil based on original occurrence data at 23 sample sites and on historical records. The upper basin has distinct highland and lowland regions, the latter including the Pantanal wetland, where "*C. ambigua*" occurs in the highlands and "*C. inflata*" occurs in both regions. At Baixo Stream in the highlands, we observed individuals with shell morphologies of either *C. ambigua* or *C. inflata*, and also individuals with intermediate shell morphology. DNA sequence variation in the upland Baixo Stream and two representative lowland populations were screened. Two mitochondrial and three nuclear genes were sequenced to test hypotheses regarding the number of species-level phylogenetic lineages present. Reported individual DNA sequences from Amazon-basin *C. ambigua* and other *Castalia* and outgroup species were included in the analysis as outgroups. Individuals from the Paraguay River basin exhibited 17 haplotypes at the mitochondrial cytochrome oxidase I (*COI*) gene and nine at mitochondrial *16S rRNA*. Analysis of haplotype networks and phylogenetic trees of combined *COI* + *16S rRNA* sequences among individuals with the respective shell morphologies supported the hypothesis that *C. ambigua* and *C. inflata* from the Paraguay River basin belong to the same species and one phylogenetic lineage. No variation was observed at the nuclear *18S rRNA* internal transcribed spacer, *28S rRNA*, or *H3NR* histone genes among individuals used in this study. Across all markers, less variation was observed among Paraguay basin populations than between Paraguay and Amazon basin populations. Our results collectively suggest that: (1) "*C. ambigua*", "*C. inflata*", and morphologically intermediate individuals within the upper Paraguay drainage represent one phylogenetic lineage, (2) a phylogeographic divide exists between *Castalia* populations occurring in the Paraguay and Amazon River basins, and (3) the evolutionary and taxonomic uncertainties that we have identified among *Castalia* species should be thoroughly assessed across their distribution using both morphological and molecular characters.

Keywords: freshwater mussels; distribution; phylogeography; Paraguay river basin; Brazil

1. Introduction

South America has a rich diversity of 168 native freshwater mussel species, with a recent description [1] and wide variation in richness among the continent's hydrogeographic regions [2–4]. Despite the important ecological services provided by freshwater mussels and the need for their conservation in the context of rapid economic development and associated ecological change, South American mussels remain largely under-studied. Conservation planning would benefit from systematic surveys of the hydrogeographic regions, recognition of habitats and environmental variables that drive the distributions of species, and a better understanding of the morphological characters that distinguish species [3].

Among South American mussels, species of the genus *Castalia* Lamarck, 1819 (Unionoida: Hyriidae) are distributed through many major basins of South America (Figure 1A). In particular, the distribution of *Castalia ambigua* Lamarck, 1819 is found in four of the eight major Brazilian basins: the Amazon, Paraguay, and Paraná, with a restricted distribution in the Uruguay River basin [5,6]. *Castalia inflata* d'Orbigny, 1835 is distributed in the Paraguay River basin and the middle-lower Parana basin, with occurrence in Argentina, Paraguay, Uruguay, and Bolivia [5,7]. However, baseline data on species' distributions are lacking in many regions.

Genus *Castalia* includes 13 [8] to 17 species [3], with the taxonomy of some members not well resolved. Species in the genus show wide morphological variation, with a particular shell shape for each different basin, hampering species recognition. Hence, genetic and phylogenetic studies are needed to differentiate similar or cryptic species, including *C. ambigua* and *C. inflata* [3]. Phenotypic variations of both valves and soft tissues were observed by D'Orbgny [9] and Ortmann [10], suggesting that specimens originating in the Amazon drainage in Bolivia should not belong to the same species reported from the Paraguay River drainage in Argentina. Five subspecies were offered by D'Orbgny [9], attributed as *C. ambigua* from the Amazon to the La Plata River drainages. The review initiated by Ortmann [10] and adopted by Bonetto [11] reported *C. ambigua ambigua* Lamarck, 1819 as restricted to the Amazon basin; *C. ambigua inflata* d'Orbigny, 1835 to the Paraguay-Paraná-La Plata basin; *C. ambigua pectinata* (Spix, 1827) to the São Francisco basin; and *C. ambigua multisulcata* Hupe, 1857 to Guyana, Venezuela, and Colombia. Of the two subspecies assigned to Argentina, *C. ambigua ambigua* and *C. ambigua inflata* [11], based on the diagnosis of shell and description of morphological characters, only *Castalia inflata* was regarded as valid taxonomically by Rumi et al. [12]. *Castalia ambigua* has multiple subspecies in some taxonomies, e.g., [2], while *C. inflata* is regarded as a species by some authors [3,13–17] and as a subspecies of *C. ambigua* by others [2,7,11,18,19]. Screenings of mitochondrial DNA of four *Castalia* species across the Amazon basin [20] showed poor phylogenetic resolution of *C. ambigua*, suggesting the possibility of cryptic variation within the nominal species. Resolution of the phylogeny of the species not only would inform taxonomic nomenclature but also conservation planning. *Castalia ambigua* is listed as a species of Least Concern in the IUCN Red List, while the status of *C. inflata* is unknown. *C. inflata* is on the Paraguayan list of endangered fauna [21].

This study focused on *Castalia* species in the upper Paraguay River basin, a region where the distributions of the respective species have not been studied intensively [22,23]. The upper Paraguay River basin has distinct regions, the highlands and lowlands, the latter including the Pantanal, the largest continuous wetland in the world [24]. We present data on the distributions of phenotypically defined "*C. ambigua*" and "*C. inflata*" in the upper Paraguay River basin, a key distributional contact zone, based on a field study of occurrence at 70 sample sites and validated historical records. At Baixo Stream in the highlands where both species occur, observation of individuals with shell morphologies intermediate between the two nominal species suggested the possibility of interbreeding. The correlation of shape and location of freshwater mussels within riverscapes has

long been recognized [25], with upland forms having thinner shells and flatter cross-sections and lowland forms having heavier shells and more inflated cross-sections. These considerations led us to frame two alternative hypotheses: (1) *Castalia ambigua* and *C. inflata* are two distinct phylogenetic lineages, perhaps with interbreeding at a zone of contact in the highlands of the Paraguay basin, and (2) *Castalia ambigua* and *C. inflata* represent one phylogenetic lineage, with the morphological variation being the consequence of morphological plasticity common along riverscapes in freshwater mussels. We tested these hypotheses by screening both mitochondrial and nuclear DNA markers within this upland population and two representative populations of *C. inflata* from the lowlands. We used published mitochondrial DNA sequences of *C. ambigua* from the Amazon basin to compare populations across a major geographic divide to better understand intraspecific variation and the phylogeographic history of the species. Using mitochondrial data, we also assessed the demographic histories of *C. ambigua* lineages.

2. Materials and Methods

2.1. Study Area and Sample Collection

The upper Paraguay River basin—with an area of 365,592 km^2 [26]—extends from the midwest of Brazil to Argentina, draining Bolivia, Paraguay, and Uruguay (Figure 1A). This riverine system connects two distinct landscapes, the highlands with most of the headwaters, and the lowlands that are marked by a seasonal flood pulse that characterizes the Pantanal, one of the world's largest continuous wetlands [24]. A sampling of freshwater mussels was conducted in the sub-basins of the Cuiabá River and the Paraguay River, in the upper Paraguay Basin inside Mato Grosso state, Brazil. We implemented nested hierarchical sampling along the hydrological gradient from highlands to lowlands, with 70 sites sampled in total (Figure 1B inset map). The capture effort was standardized at 1 person-hour sampling quadrats within transects. Individual mussels were collected, measured, tagged, and returned to the same place in the river or lake.

2.2. Biometrical Measurements

All *C. ambigua* (n = 200) and *C. inflata* (n = 557) individuals were measured with a digital caliper at a resolution of 0.01 mm. The characters measured were total length (*Lt*, mm), height (*h*, mm), and width (*wi*, mm). To characterize groups, all data were standardized to have a mean of zero and deviation of 1, transforming the data on the same scale of variation, as suggested by Gotelli and Ellison [27]. Then, the data were ordered through Principal Components Analysis (PCA) using the software R [28]. For a graphical representation of the results of the PCA, we used the *autoplot* function of the package "*ggfortify*" [29].

2.3. Molecular and Phylogenetic Analyses

After observing individuals with shell morphologies intermediate between *C. ambigua* and *C. inflata* at Baixo Stream in the highlands, we resolved to test alternative phylogenetic hypotheses by screening mitochondrial and nuclear DNA markers in individuals from this stream and from other populations. Samples for molecular genetic and phylogenetic analyses were collected by hand at the three sites (Table 1, red numbers in Figure 1B inset map) in November 2015. Tissue samples from the mantle were obtained from 71 individuals: 34 from Baixo Stream (14°40′45.7″ S, 56°14′10.0″ W, site 1 on Figure 1B inset map), 10 from Valo Verde Lake (15°49′19.0″ S, 56°07′44.48″ W, site 2 on Figure 1 inset map), and 27 from Claro Stream (16°36′21.84″ S 56°43′31.67″ W, site 3 on Figure 1B inset map). *Castalia inflata* was collected at all three sites. At Baixo Stream, 19 mussels were classified as *C. ambigua* in the field, 44 as *C. inflata*, and 8 as "*C. ambigua*-like", i.e., morphologically intermediate between *C. ambigua* and *C. inflata*. Thus, "*C. ambigua*-like" individuals were collected only at Baixo Stream. After gently prying each mussel partially open, the tip of a sterilized scissor was used to non-lethally remove a small

sample of mantle tissue [30]. The tissue sample was fixed in 70% ethanol at ambient temperature. Samples were transported for subsequent analysis at Virginia Tech, Blacksburg, VA, USA.

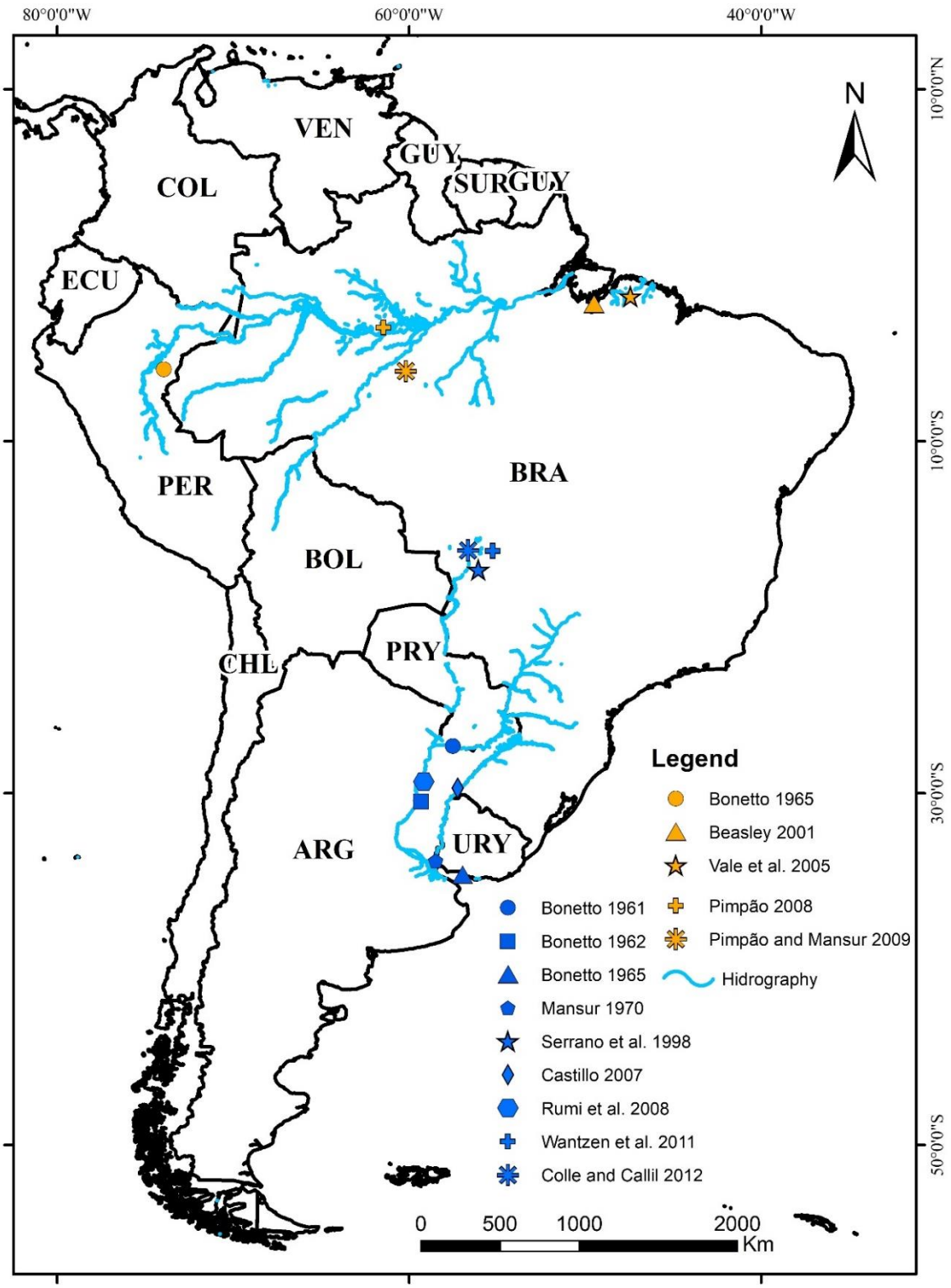

(**A**)

Figure 1. *Cont*.

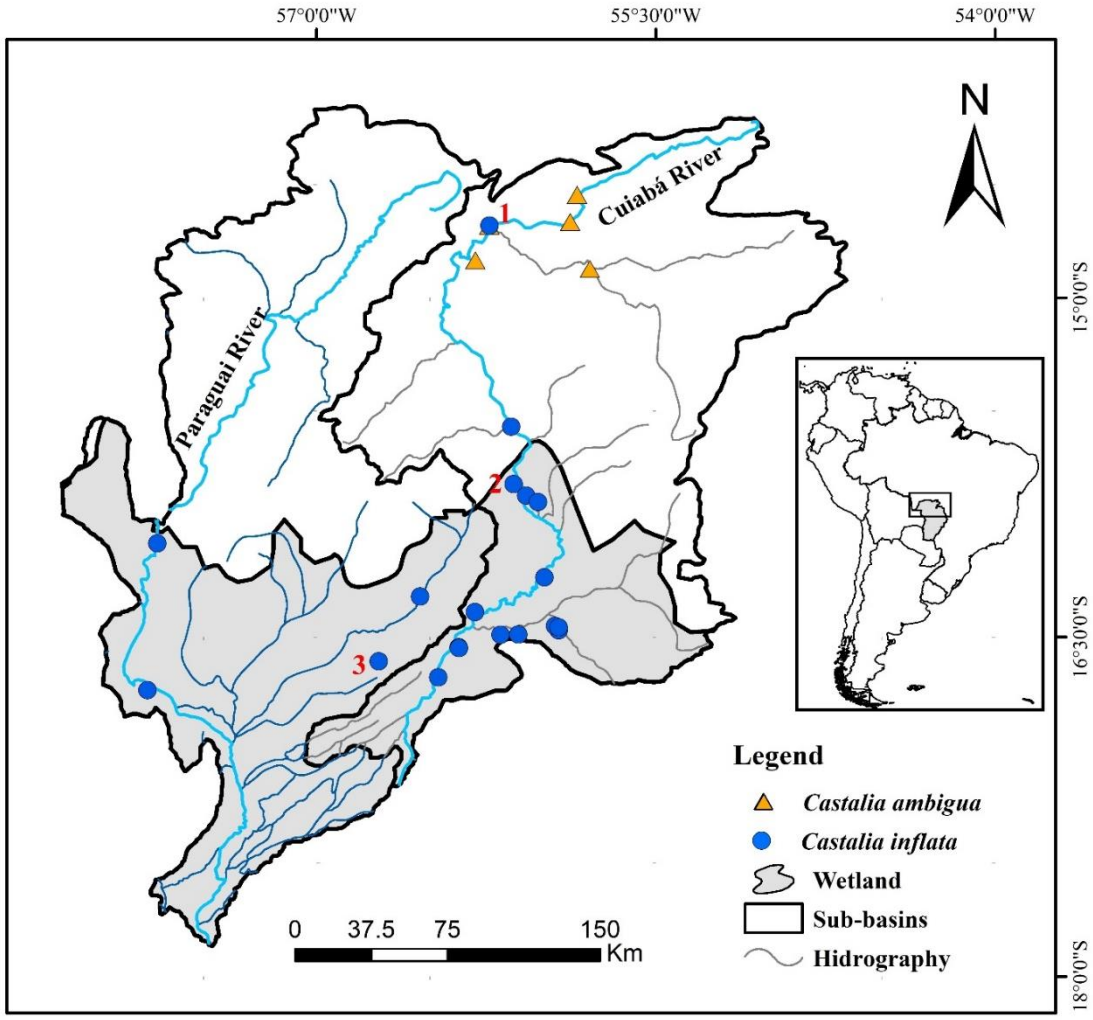

(**B**)

Figure 1. Locations of past and present studies of Castalia species. (**A**). Chronology of registered occurrences of *Castalia ambigua* Lamarck, 1819 and *Castalia inflata* d'Orbigny, 1835 in South America. Orange symbols denote *C. ambigua* and blue denote *C. inflata*. The Amazon basin is to the north, and the Paraguay basin to the south. References: Bonetto 1961 [5], Bonetto 1962 [31], Bonetto 1965 [11], Mansur 1970 [7], Serrano et al. 1998 [32], Castillo 2007 [33], Wantzen et al. 2011 [34], Colle and Callil [22], Beasley 2001 [35], Vale et al. 2005 [6], Rumi et al. 2008 [12], Pimpao et al. 2008 [36], and Pimpao and Mansur 2009 [37]. (**B**). Locations of occurrence and sample sites for *Castalia ambigua* Lamarck, 1819 (orange triangles) and *Castalia inflata* d'Orbigny, 1835 (blue dots) within the upper Paraguay River basin in this study. Red numerals indicate sample sites for molecular analysis: 1—Baixo Stream (both *C. ambigua* and *C. inflata*); 2—Valo Verde Lake; and 3—Claro River. Lack of shading indicates upland areas; gray shading indicates lowland areas.

Table 1. Collection sites for *Castalia* specimens in the upper Paraguay river basin; "x" denotes the occurrence of specimens expressing the phenotype of that species.

	Lake or River	Latitude	Longitude	*Castalia inflata* d'Orbigny, 1835	*Castalia ambigua* Lamarck, 1819	Occurrence
1	Cuiabazinho River	14°32′35.48″ S	55°50′53.49″ W	-	x	Highlands
2	Cuiabazinho River	14°39′46.63″ S	55°52′45.30″ W	-	x	Highlands
3	APM Manso	14°52′16.89″ S	55°47′31.27″ W	-	x	Highlands
4	Baixo Stream	14°40′46.39″ S	56°14′9.72″ W	x	x	Highlands
5	Cuiabá River	14°49′59.78″ S	56°17′53.34″ W	-	x	Highlands
6	Cuiabá River	15°34′08.25″ S	56°08′23.02″ W	x	-	Lowlands
7	Valo Verde oxbow lake	15°49′20.36″ S	56° 7′43.59″ W	x	-	Lowlands
8	Cuiabá River	15°52′26.66″ S	56° 4′25.09″ W	x		Lowlands
9	Poço oxbow lake	15°54′06.73″ S	56°01′17.20″ W	x	-	Lowlands
10	Paraguay River	16°05′08.60″ S	57°42′18.65″ W	x	-	Lowlands
11	Corixo das Conchas oxbow lake	16°28′6.075″ S	55°55′49.837″ W	x	-	Lowlands
12	Coqueiro oxbow lake	16°23′19.11″ S	56°18′00.57″ W	x	-	Lowlands
13	Jacaré (Ninhal) oxbow lake	16°14′08.89″ S	55°59′37.10″ W	x	-	Lowlands
14	Bento Gomes River	16°19′13.49″ S	56°32′36.21″ W	x	-	Lowlands
15	Pombas oxbow lake	16°26′54.07″ S	55°56′45.30″ W	x	-	Lowlands
16	Conchas oxbow lake	16°27′18.80″ S	55°55′46.40″ W	x	-	Lowlands
17	Serragem oxbow lake	16°29′14.80″ S	56°06′31.30″ W	x	-	Lowlands
18	Barco Velho oxbow lake	16°29′18.00″ S	56°11′13.15″ W	x	-	Lowlands
19	Cuiabá River	16°32′36.45″ S	56°22′20.90″ W	x	-	Lowlands
20	Oxbow lakes	16°32′49.20″ S	56°18′12.00″ W	x	-	Lowlands
21	Claro Stream	16°36′21.84″ S	56°43′31.67″ W	x	-	Lowlands
22	Santa Rosa oxbow lake	16°40′33.20″ S	56°27′45.30″ W	x	-	Lowlands
23	Descalvado oxbow lake	16°44′00.29″ S	57°44′55.67″ W	x	-	Lowlands

The DNA was isolated from preserved tissue using the DNeasy Blood and Tissue Kit (Qiagen, Germantown, MD, USA). DNA quality and quantity were assessed using a µLite PC spectrophotometer (Biodrop, Cambridge, UK). The DNA concentration of samples was diluted to 10–30 ng/µL. We amplified two mitochondrial genes, cytochrome oxidase I (*COI*) and *16S rRNA*, and three nuclear (internal transcribed sequence *ITS-1* of *18S rRNA*, *28S rRNA*, and histone *H3NR*) DNA sequences. The PCR primers used for amplification of targeted sequences are shown in Table 2. Polymerase chain reactions (PCR) were performed in a final volume of 22 µL, containing 0.1 µL *Taq* polymerase (5 units/µL) (Promega, Madison, WI, USA), 2 µL of 5× buffer, and 2 µL $MgCl_2$ (25 mM), 0.4 µL bovine serum albumin (BSA, 1 mg/mL), 0.4 µL of all four 5 mM dNTPs, 0.4 µL each of the respective two 5 µM primer solutions, 14.5 µL sterile ultrapure water (EMD Millipore, Darmstadt, Germany), and 1 µL of template DNA. The PCR was conducted in Bio-Rad thermocyclers, either a T100 or MyCycler. In the case of *COI* and *H3*, the PCR protocol was 3 min at 94 °C; 35 cycles of: one min at 94 °C, 45 s at 55 °C, 1 min at 72 °C; and a final extension at 72 °C for 5 min. For *16S* and *18S ITS*, the PCR started with 3 min at 94 °C; followed by 35 cycles of 40 s at 94 °C, 40 s of 53 °C (for *16S*) or 60 °C (*18S ITS*), one min at 72 °C; and a final extension for 5 min at 72 °C. For amplification of the *COI* gene, we ran two PCR reactions, each of them with different forward primers but the same reverse primer. Finally, the *28S* PCR reactions (22-µL) included 2.2 µL DNA extract, 0.1 µL Promega *Taq* polymerase, 2 µL 10× buffer and 2 $MgCl_2$, 0.4 µL BSA (1 mg/mL), 0.4 µL of all four 5 mM dNTPs, 0.4 µL each of the two 5 µM primer solutions, and 13.3 µL sterile ultrapure water. PCR protocols were carried out in the previously mentioned thermocyclers and included: 3 min at 94 °C; 35 cycles of: one min at 94 °C, one min at 53 °C, and 90 s at 72 °C; and five min at 72 °C.

Table 2. PCR primers used for amplification of genetic markers screened in this study.

Gene, Primer	Primer Name	Primer Sequence (5′ to 3′)	Reference
COI F	LCO1490	GGT CAA CAA ATC ATA AAG ATA TTG G	[38]
COI F	COIF	GTT CCA CAA ATC ATA AGG ATA TTG G	[39]
COI R	HCO700dy2	TCA GGG TGA CCA AAA AAY CA	[40]
16S F	16SL1987	GCC TCG CCT GTT TAC CAA AAA C	[41]
16S R	16Sbr-H	CCG GTC TGA ACT CAG ATC ACG	[42]
18S ITS F	ITS1A	AAA AAG CTT TTG TAC ACA CCG CCC GTC	[43]
18S ITS R	ITS1B	AGC TTG CTG CGT TCT TCA TCG A	[43]
28S F	D23F	GAG AGT TCA AGA GTA CGT G	[44]
28S R	D4RB	TGT TAG ACT CCT TGG TCC GTG T	[44]
H3 F	H3F	ATG GCT CGT ACC AAG CAG ACV GC	[45]
H3 R	H3R	ATA TCC TTR GGC ATR ATR GTG AC	[45]

The presence of amplification product of a size appropriate for the respective gene regions used in our study was confirmed using standard gel electrophoresis through a 2% agarose TBE (tris-borate-EDTA) gel, which was stained with ethidium bromide. PCR reaction products were sequenced using both forward and reverse primers with the BigDye Terminator Cycle Sequencing Kit v.3.1 on an ABI3730 DNA sequencer at the Fralin Life Sciences Institute (Blacksburg, VA, USA). Consensus sequences were obtained by using Geneious 7.0.6 (Biomatters, Auckland, New Zealand). GeneStudio Professional Edition, ver. 2.2.0.0 (Informer Technologies, Inc., Los Angeles, CA, USA) was used to align the sequences. All consensus sequences for *C. ambigua* and *C. inflata* were aligned within and between the species and any putative polymorphisms were cross-checked against the original chromatogram to remove any reading errors. Our *18S ITS* sequences were aligned using both Clustal W [46] and webPRANK [47] alignment software. The resulting gaps were coded using FastGap v1.2 [48]. Original DNA sequences were submitted to GenBank using the BanKlT sequence submission tool (http://www.ncbi.nlm.nih.gov/WebSub/?tool=genbank). DNA sequences in our original .fasta files were compared against entries in GenBank (http://www.ncbi.nlm.nih.gov/nuccore/) using the Basic Local Alignment Search Tool [49]. All archived sequences returned with homology scores over 90% were recorded.

Variable sites and genetic variability of mitochondrial DNA sequences were assessed using DnaSP 5.10 [50], including number of haplotypes, the average number of nucleotides differences, gene diversity, and nucleotide diversity for each species at each sampling location for the *COI* and *16S* gene regions.

Haplotype networks for each marker were constructed using PopArt (Population Analysis with Reticulate trees) [51] to show the distribution of the haplotypes among the three populations and among the three species. All haplotype networks were constructed using the TCS inference method [52].

We conducted phylogenetic analyses of the DNA sequences from *C. ambigua* sampled in this study and outgroup species within Tribes Castaliini and Hyriini downloaded from GenBank. The *COI* sequences included those from our own results for *Castalia* sp. (GenBank accession numbers KY474356-KY474356-372), *C. ambigua* (KU888236-KU888243), and *Triplodon corrugatus* (KU888253) from da Cruz Santos-Neto et al. [20]. The *16S* sequences analyzed included *Castalia* sp. (KU463457-KU463465) from this study, as well as archived sequences from *C. ambigua* (KU888207-KU888213) and *Triplodon corrugatus* (KU888224). The *18S ITS* sequences included *Castalia* sp. (KY463466) from our study, plus *C. ambigua* (KU888178-888182), *C. stevensi* (KU88184), and *Callonaia duprei* (KU888175) from da Cruz Santos-Neto et al. [20]. For *COI* + *16S*, the outgroup was *Triplodon corrugatus* (KU888253 + KU888224). The evolutionary model for each sequence alignment was selected using Kakusan4 [53], where we used Akaike information Criterion (*AIC*) to find the most appropriate theoretical model of molecular evolution. Using that model, maximum likelihood phylogenetic trees were constructed using MrBayes 3.2.5 [54]. Bayesian analysis included four (*16S*, *COI* + *16S*) and eight (*COI* and *18S ITS*) Markov chain Monte Carlo chains with a total of 600,000, 500,000, 500,000, and 1.5 million generations for *COI*,

16S, *18S ITS*, and *COI + 16S*, respectively, with trees sampled every 100 generations. Tree topologies remaining after the first 25% were excluded from the cold chain and were used to calculate posterior node probabilities [55]. We used Tracer v. 1.6.0 [56] to assess MCMC convergence and to ensure that the effective sample size (ESS) was higher than 200. For each dataset, we assessed species delimitation using the Automatic Barcode Gap Discovery (ABGD) [57] method which detects barcode gaps, where we used the Kimura distance model, a minimum intraspecific distance of 0.01, and a maximum intraspecific genetic distance of 0.1. The final phylogenetic tree was created by using the consensus trees in RStudio using "ape" [58], and "phytools" [59] packages.

2.4. Inference of Historical Demography

We tested two demographic scenarios using Approximate Bayesian Computation (ABC) modeling as implemented in DIYABC [60]. Noting that our mitochondrial DNA phylogenetic analysis identified two distinct lineages for *C. ambigua*, one in the Amazon River basin and the other in the Paraguay River basin (see Results), Scenario 1 was designated as the null model, where all four populations diverged at the same time from a common ancestor with equal divergence rates (Figure 2, left). Scenario 2 assumed the Paraguay and Amazon basin lineages of *C. ambigua* diverged initially from each other earlier in time (t_2), and then later (t_1) the three populations in the Paraguay River basin diverged simultaneously from their common ancestor with equal divergence rates. Using combined mitochondrial DNA sequences, we simulated historical demography over millennial (e.g., >1000 years ago) time-scales. Each scenario contained all four extant populations at generation t_0 (Figure 2, right). We conducted simulations assuming all populations diverged simultaneously from a common ancestral population.

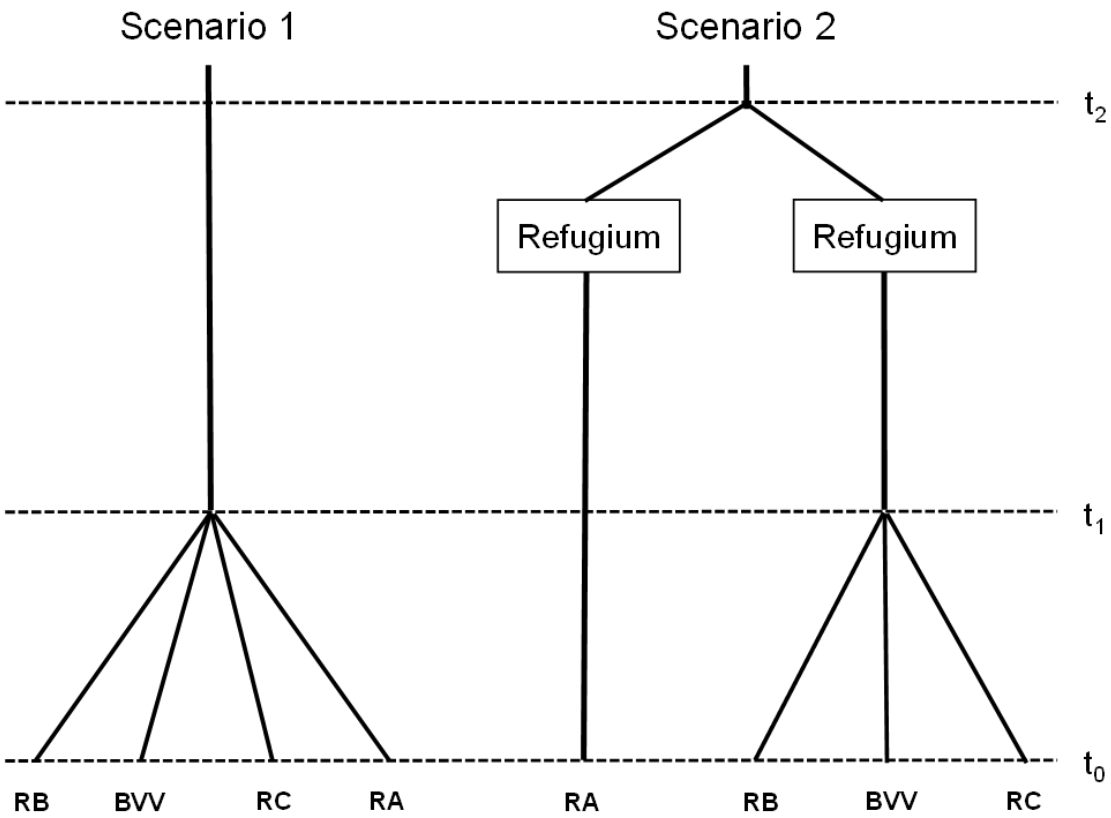

Figure 2. The two demographic scenarios tested for populations of *C. ambigua* in the Amazon River and Paraguay River basins of Brazil using DIYABC [59,60]. Each scenario assumes four extant populations at t_0, where RB = Baixo Stream, BVV = Valo Verde Lake, RC = Claro Stream, and RA = Amazon River, populations, respectively, and that they diverged from each other at some point in the past. Divergence time-points t_1 and t_2 are displayed on right.

Prior values of N_e for extant and ancestral populations ranged from a minimum of 10 individuals to a maximum of 50,000 individuals and utilized a uniform distribution (Table 3). The N_e values were based on preliminary analyses to confirm the upper boundaries of the prior values. The prior value for time-point t_1 was 10–20,000 generations ago and for t_2 1000–100,000 generations ago, with both time-points utilizing a uniform distribution. Mean generation time was set at 5.5 years for both species based on female longevity of 10 years, which was derived from a life-table analysis of demographic data for the Baixo Stream population of *C. ambigua* (C. Callil, unpublished data). To estimate the mean mutation rate, we used a Hasegawa–Kishino–Yano mutation model [61] and set the per-site per-generation mutation rate to range from a minimum rate of 1×10^{-8} to a maximum of 1×10^{-6}. For each demographic scenario, two million simulations were run, and then their respective posterior probabilities were compared using logistic regression to determine the most probable scenario [62]. Finally, confidence in each scenario was assessed by evaluating Type I and Type II error rates [60]. One thousand test data sets were simulated using each scenario, respectively, and then the posterior probabilities were evaluated for the simulated data sets. The Type I error rate was calculated from the proportion of posterior probabilities of Scenario I that were lower than the posterior probabilities of Scenario II when Scenario I was the true scenario, and vice versa for Scenario II. The Type II error rate was calculated from the proportion of posterior probabilities of Scenario I that were higher than the posterior probabilities of Scenario II when Scenario I was not the true scenario, and vice versa for Scenario II.

Table 3. Scenario 2 prior distributions of parameters and median posterior parameter values for populations of *C. ambigua* in the Amazon River and Paraguay River basins, Brazil.

River Population	Parameter	Prior Distributions			Posterior Distributions		
		Min.	Max.	Distribution	Median	95% Credible Interval	
Baixo Stream	N_e	10	50,000	Uniform	7660	1880	31,200
Valo Verde Lake	N_e	10	50,000	Uniform	4020	1130	15,900
Claro Stream	N_e	10	50,000	Uniform	28,800	10,400	47,100
Amazon River	N_e	10	50,000	Uniform	32,600	13,500	48,100
Ancestral	N_e	10	100,000	Uniform	77,800	37,700	98,000
	T_1 (generations)	10	20,000	Uniform	1290	366	6080
	T_2 (generations)	1000	100,000	Uniform	7240	2830	9750
	Mutation rate (μ)	1×10^{-8}	1×10^{-6}	Uniform	6.64×10^{-7}	3.64×10^{-7}	9.5×10^{-7}

2.5. Permits and Ethical Aspects

We obtained authorization from IBAMA, the Brazilian Institute of the Environment and Renewable Natural Resources, for the collection of zoological material in accordance with Portaria do lbama n° 332/90 and other relevant rules and regulations.

3. Results

3.1. Morphology and Distribution

The genus *Castalia* has thick shells of an equilateral triangular shape, the umbos are high and prominent with umbonal sculpture well developed and extending over a large part of the shell, the posterior ridge is sharp, and the anterior shell margin is well defined and ligament well developed [63]. Data from individuals collected at 70 sample sites in the upper Paraguay River basin showed that *C. ambigua* occurred at 5 sites (Table 1, Figure 1B, inset map) and *C. inflata* at 19.

Castalia inflata was associated with the lowlands, marginal shallow lakes, and oxbow lakes of the Cuiabá River in areas influenced by the spring flood pulse [22,23]. *Castalia inflata* (Figure 3A, top row) has an equilateral triangular shell; very inflated; high and robust; rounded anterior border;

obliquely truncated posterior margin, forming an edge with a ventral border that is straight at the posterior region; umbos central, tall, large and wide; radial umbonal sculpture formed by parallel rays strongly marked, generally covering the entire surface of the shell; keel high and prominent, with a very strong back slope; shield large and flat, periostracum matte dark-brown; hinge strong, very arched and broad, with pseudocardinal and lateral teeth perpendicularly striped [64].

Castalia ambigua found exclusively in the highland streams with a fast flow and high productivity in limestone-dominated watersheds [22,23]. *Castalia ambigua* (Figure 3B, middle row) has an inequilaterally triangular shell; inflated; high and robust; rounded anterior border and slightly tapered; obliquely truncated posterior margin forming an edge with a ventral margin that is straight or rounded at the posterior third; umbos sub-central, lower and smaller; radial umbonal sculpture formed by strongly marked diverging rays, usually longer posteriorly; keel high and a little rounded, with oblique dorsal slope, shield small and elongated; periostracum matte brown; hinge strongly arched and wide; pseudocardinal and lateral teeth perpendicularly striped [36,64].

As noted above, at Baixo Stream in the highlands, "*C. ambigua*-like" individuals were observed (Figure 3C, bottom row) that exhibited morphological traits intermediate to those described for nominal *C. inflata* and *C. ambigua*.

Figure 3. Shell morphologies for representative *C. inflata* (**A**, top row), *C. ambigua* (**B**, middle row), and "*C. ambigua*-like" (**C**, bottom row). Bars indicate 1 cm.

3.2. Biometry

A total of 557 *C. inflata* individuals from 19 sample sites were measured, with a mean (±SE) length of 27.22 ± 5.59 mm, width of 18.69 ± 4.17 mm, and height of 24.59 ± 5.24 mm. A total of 200 *C. ambigua* individuals from five different sites were measured. Variation was higher for *C. ambigua*, with a mean length of 39.11 ± 12.47 mm, width of 19.94 ± 6.46 mm, and height of 37.76 ± 10.32 mm.

Results of principal components analysis (Figure 4) showed two distinct groups, one for each nominal species, with 92.88% of the variance explained by the first axis. Some degree of overlap among the groups is visible (Figure 3A), which may be the consequence of the morphometric variation of individuals with intermediate morphology, hereafter "*C. ambigua*-like" individuals. The biometrical variable that contributed most greatly to variation was width (Figure 4).

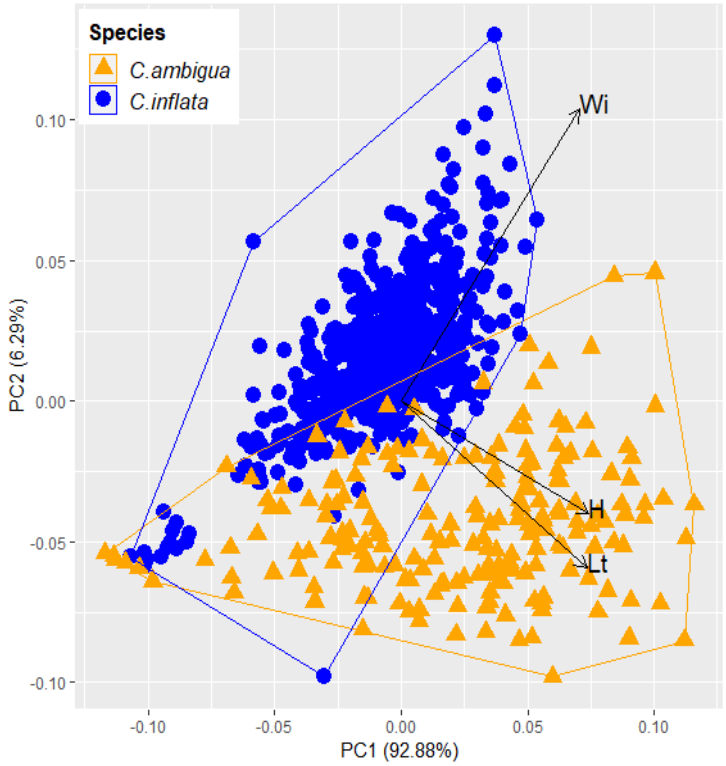

Figure 4. Ordination by principal coordinates analysis of biometrical variables of morphology designated as *C. inflata* (blue dots) and *C. ambigua* (orange dots) from the Upper Paraguay River Basin.

3.3. Molecular and Phylogenetic Analyses

A total of 71 samples—34 from Baixo Stream (highlands), 27 from Claro Stream (lowlands), and 10 from Valo Verde Lake (lowlands)—were sequenced at the *COI* gene, 19 that were morphologically *C. ambigua*, eight "*C. ambigua*-like" or intermediate, and 44 *C. inflata*. We considered molecular variation among *C. ambigua* from the Amazon River watershed [20] as a geographical outgroup. Among the sequence alignments, 25 haplotypes were identified on the basis of 25 variable nucleotides within 514 bp (Table 4). The respective haplotypes are reported as GenBank accession numbers indicated in Table 4. Metrics of genetic variation at the mitochondrial *COI* region (Table 5) show higher numbers of nucleotide differences (k) and nucleotide diversity (π) among *C. ambigua*-like than among *C. ambigua* or *C. inflata* individuals within the Paraguay River watershed despite the smaller sample size. Haplotype diversity (h) was somewhat higher in *C. ambigua* than in *C. inflata*. *COI* sequences for *C. ambigua*, *C. inflata*, and *C. ambigua*-like individuals were 91%, 92%, and 93% similar to the *Callonaia duprei* (Recluz, 1842), respectively, and 93%, 94%, and 95% similar to the *Castalia quadrata* (Sowerby, 1867) reference sequences retrieved from GenBank.

Table 4. Haplotypes for *Castalia* sp. at the mitochondrial cytochrome oxidase I (*COI*) gene. Haplotypes *Cast_COI*_01 through 17 are original data from the Paraguay River basin; *C. ambigua* 1 through 8 are from the Amazon River basin and were collected by da Cruz Santos-Neto et al. [20]. Numbers refer to nucleotide position.

	25	**28**	**31**	**34**	**40**	**47**	**49**	**51**	**52**	**55**	**61**	**64**	**67**	**70**	**73**	**85**	**118**	**139**	**148**	**154**	**163**	**169**	**172**
Cast COI 01	G	G	A	A	G	C	T	G	G	A	C	A	A	G	G	A	G	G	G	T	G	A	G
Cast COI 02	.	.	.	.	.	.	.	.	.	.	.	.	G	.	.	.	.	.	.	.	.	.	.
Cast COI 03	.	.	.	.	.	.	.	.	.	.	.	.	G	.	.	.	.	.	.	.	.	.	.
Cast COI 04	.	.	.	.	.	.	.	.	.	.	.	.	G	.	.	.	.	.	.	.	.	.	.
Cast COI 05	.	.	.	.	.	.	.	.	.	.	.	.	G	.	.	.	.	.	.	.	.	.	.
Cast COI 06	.	.	.	.	.	.	.	.	.	.	.	.	G	A	.	.	.	.	.	.	.	.	.
Cast COI 07	.	.	.	.	.	.	.	.	.	.	.	.	G	A	.	.	.	.	.	.	.	.	.
Cast COI 08	.	.	.	.	.	.	.	.	.	.	.	.	G	A	.	.	.	.	.	.	.	.	.
Cast COI 09	.	.	.	.	.	.	.	.	.	.	.	.	G	A	.	.	.	.	.	.	.	.	.
Cast COI 10	.	.	.	.	.	.	.	A	.	.	.	.	G	A	.	.	.	.	.	A	.	.	.
Cast COI 11	.	.	.	.	A	.	.	.	.	.	.	.	G	A	.	.	.	.	.	.	.	.	.
Cast COI 12	.	.	.	.	.	.	.	.	.	.	.	.	G	.	.	.	.	.	.	.	.	.	.
Cast COI 13	.	.	.	.	.	.	.	.	.	.	.	.	G	A	.	.	.	.	.	.	.	.	.
Cast COI 14	.	.	.	.	.	.	.	.	.	.	.	.	G	.	.	.	.	.	.	.	.	.	A
Cast COI 15	.	.	.	.	.	.	.	.	.	.	.	.	G	.	.	.	.	.	.	.	.	.	.
Cast COI 16	.	.	.	.	.	.	.	.	.	.	.	.	G	.	.	.	.	.	.	.	.	.	.
Cast COI 17	.	.	.	.	.	.	.	.	A	.	.	.	G	.	.	.	.	.	.	.	.	.	.
Castalia ambigua 1	A	.	G	G	.	.	.	.	.	G	G	.	G	.	.	.	.	.	.	.	A	G	.
Castalia ambigua 2	A	.	G	G	.	.	.	.	.	G	G	.	G	.	.	.	.	.	.	.	A	G	.
Castalia ambigua 3	A	.	G	G	.	.	.	.	.	G	G	.	G	.	.	.	.	.	.	.	A	G	.
Castalia ambigua 4	A	.	G	G	.	.	.	.	.	G	G	.	G	.	.	.	.	.	.	.	A	G	.
Castalia ambigua 5	.	.	G	.	.	.	.	.	.	G	G	G	G	.	.	G	.	A	.	.	A	G	.
Castalia ambigua 6	.	.	G	.	.	.	.	.	.	G	G	G	G	.	.	G	.	A	.	.	A	G	.
Castalia ambigua 7	.	T	.	G	.	T	A	.	.	G	G	G	.	A	A	.	A	A	A	.	.	G	.
Castalia ambigua 8	.	T	.	G	.	T	A	.	.	G	G	G	.	A	A	.	A	A	A	.	.	G	.

Table 4. *Cont.*

	181	**187**	**192**	**193**	**199**	**211**	**229**	**253**	**259**	**260**	**262**	**265**	**268**	**278**	**289**	**295**	**310**	**316**	**320**	**328**	**335**	**337**	**361**
Cast COI 01	A	G	C	T	T	T	G	G	A	T	A	A	G	G	A	G	G	T	T	T	G	T	G
Cast COI 02	.	.	.	.	.	.	.	.	.	.	.	.	.	.	.	.	.	.	.	.	.	.	.
Cast COI 03	.	.	.	.	.	.	.	.	.	.	.	.	.	.	.	.	.	.	.	.	.	.	.
Cast COI 04	.	.	.	.	.	.	.	.	.	.	.	.	.	.	.	.	.	.	.	.	.	.	.
Cast COI 05	.	.	.	.	.	.	.	.	.	.	.	.	.	A	.	.	.	.	.	.	.	.	.
Cast COI 06	.	A	.	.	.	.	.	.	.	C	.	G	.	.	.	.	.	.	.	C	.	.	.
Cast COI 07	.	A	.	.	.	.	.	.	.	C	.	G	.	.	.	.	.	.	.	C	.	.	.
Cast COI 08	.	A	.	.	.	.	.	.	.	C	.	G	.	.	.	.	.	.	.	C	.	.	.
Cast COI 09	G	A	.	.	.	.	.	.	.	C	.	G	.	.	.	.	.	.	.	C	.	.	.
Cast COI 10	.	A	.	.	.	.	.	.	.	C	.	G	.	.	.	.	.	.	.	C	.	.	.
Cast COI 11	.	A	.	.	.	.	.	.	.	C	.	G	.	.	.	.	.	.	.	C	.	.	.
Cast COI 12	.	.	T	.	.	.	.	.	.	.	.	.	.	.	.	.	.	.	.	.	.	.	.
Cast COI 13	.	A	.	.	.	.	.	.	.	.	.	G	.	A	.	.	.	.	.	.	.	.	.
Cast COI 14	.	A	.	.	.	.	.	.	.	C	.	G	.	.	.	.	.	.	.	C	.	.	.
Cast COI 15	.	.	.	.	.	.	.	.	.	.	.	.	.	.	.	.	.	.	.	.	.	.	.
Cast COI 16	.	.	.	.	.	.	.	.	.	.	.	.	.	.	.	.	.	.	.	.	.	.	.
Cast COI 17	.	.	.	.	.	.	.	.	.	.	.	.	.	.	.	.	.	.	.	.	.	.	.
Castalia ambigua 1	.	.	.	.	.	.	A	.	.	.	G	.	A	.	T	A	.	C	.	.	T	.	A
Castalia ambigua 2	.	.	.	.	.	.	A	.	.	.	G	.	A	.	T	A	.	C	.	.	T	.	A
Castalia ambigua 3	.	.	.	.	.	.	A	.	.	.	G	.	A	.	T	A	.	C	.	.	T	C	A
Castalia ambigua 4	.	.	.	.	.	.	A	.	.	.	G	.	A	.	T	A	.	C	.	.	T	C	A
Castalia ambigua 5	.	.	.	.	C	.	.	.	.	.	.	.	A	.	T	A	.	A	C	.	.	C	A
Castalia ambigua 6	.	.	.	.	C	.	.	.	.	.	.	.	A	.	T	A	.	A	C	.	.	C	A
Castalia ambigua 7	.	.	.	C	.	A	.	A	G	.	G	.	.	.	T	.	A	.	.	.	.	.	.
Castalia ambigua 8	.	.	.	C	.	A	.	A	G	.	G	.	.	.	T	.	A	.	.	.	.	.	.

Table 4. *Cont.*

	376	379	388	397	406	424	430	442	451	457	463	467	491	535	*C. ambigua*	*C. inflata*	*C. ambigua*-like	Rio Baixo	Baia Valo Verde	Rio Claro	Rio Amazonas	Accession Number
Cast COI 01	G	T	A	A	G	C	T	T	G	G	A	A	G	T		1			1			KY474356
Cast COI 02	.	.	.	.	.	.	.	.	.	.	.	.	.	.		23			5	18		KY474357
Cast COI 03	.	.	.	.	.	.	.	C	.	.	.	.	.	.	1	8		1	3	5		KY474358
Cast COI 04	.	.	.	.	.	.	.	C	.	.	.	.	A	.		1			1			KY474359
Cast COI 05	.	.	.	.	.	.	.	C	.	.	.	.	.	.	6	6	4	16				KY474360
Cast COI 06	.	.	.	.	.	.	.	C	.	.	.	.	.	.	4	1		5				KY474361
Cast COI 07	.	.	.	.	.	.	.	C	.	.	.	.	.	G	2		1	3				KY474362
Cast COI 08	.	.	.	.	.	.	.	C	.	A	.	.	.	.	1			1				KY474363
Cast COI 09	.	.	.	.	.	.	.	C	.	.	.	.	.	.	1			1				KY474364
Cast COI 10	.	.	.	.	.	.	.	C	.	.	.	.	.	.	1			1				KY474365
Cast COI 11	.	.	.	.	.	.	.	C	.	.	.	.	.	.	2		2	4				KY474366
Cast COI 12	.	.	.	.	.	.	.	C	.	.	.	.	.	.			1	1				KY474367
Cast COI 13	.	.	.	.	.	.	.	C	.	.	.	.	.	.	1			1				KY474368
Cast COI 14	.	.	.	.	.	.	.	.	.	.	.	.	.	.		1				1		KY474369
Cast COI 15	A	.	.	G	.	.	.	C	.	.	.	.	.	.		1				1		KY474370
Cast COI 16	A	.	.	.	.	.	.	C	.	.	.	.	.	.		1				1		KY474371
Cast COI 17	.	.	.	.	.	.	.	C	.	.	.	.	.	.		1				1		KY474372
Castalia ambigua 1	A	C	.	G	.	T	C	.	.	.	.	.	-	-	1						1	KU888236
Castalia ambigua 2	A	C	.	G	.	T	C	.	.	.	.	.	-	-	1						1	KU888237
Castalia ambigua 3	A	C	.	.	.	T	C	.	.	.	.	.	-	-	1						1	KU888238
Castalia ambigua 4	A	C	.	.	.	T	C	.	.	.	.	.	-	-	1						1	KU888239
Castalia ambigua 5	A	C	G	.	.	T	G	.	.	T	.	G	-	-	1						1	KU888240
Castalia ambigua 6	A	C	G	.	.	T	G	.	.	T	.	G	-	-	1						1	KU888241
Castalia ambigua 7	A	.	.	.	A	T	.	.	A	T	G	.	-	-	1						1	KU888242
Castalia ambigua 8	A	.	.	.	A	T	.	.	A	T	G	.	-	-	1						1	KU888243

Table 5. Variation at the mitochondrial *COI* region for *Castalia* species among three sites in the upper Paraguay River basin and one site in the upper Amazon basin of Brazil.

Species	Collection Area	*n*	Number of Haplotypes	Average Number of Nucleotide Differences (*k*)	Haplotype Diversity (*h*)	Nucleotide Diversity (π)
C. ambigua	Baixo Stream	19	9	3.81	0.865	0.007
C. inflata	Baixo Stream	7	2	1.71	0.286	0.003
C. ambigua-like	Baixo Stream	8	4	4.18	0.750	0.008
C. inflata	Valo Verde Lake	10	4	0.93	0.711	0.002
C. inflata	Claro Stream	27	6	1.09	0.536	0.002
C. ambigua	Amazon River	8	4	18.29	0.857	0.040

Because the *COI* sequences from da Cruz Santos-Neto et al. [20] are shorter than ours, after trimming ours to an equal length of 343 base pairs, some of our haplotypes became the same as others. Sequences that became identical after trimming were *Cast_COI*_06 with *Cast_COI*_07, and *Cast_COI*_03 with *Cast_COI*_04. Some sequences reported by da Cruz Santos Neto et al. [18] were found to be the same haplotype, *viz*. KU888238 with KU8888239, KU888236 with KU888237, KU888240 with KU888241, and KU888242 with KU888243. Considering the haplotypic distribution on a geographical basis (Figure 5A), the Claro Stream collection exhibited haplotypes *Cast_COI*_2, 3, 14, 15, 16, and 17, the Valo Verde Lake collection haplotypes *Cast_COI*_1, 2, 3, and 4, and the Baixo Stream collection haplotypes *Cast_COI*_3, 5, 6, 7, 8, 9, 10, 11, 12, and 13. Claro Stream and Vale Verde Lake haplotypes tended to the left of the haplotype network and Baixo Stream haplotypes to the right, reflecting geographic and elevational distributions. Most striking, the Amazon River haplotypes are at least 18 mutational steps separated from the Rio Paraguay haplotypes. Considering haplotypes on a taxonomic basis (Figure 5B), some haplotypes (*Cast_COI*_3, 5, and 6) were exhibited across nominal species, and *C. inflata* haplotypes were embedded among the *C. ambigua* haplotypes. That is, haplotypes *Cast_COI*_1, 2, 4, 14, 15, 16, and 17 were observed only in *C. inflata*, haplotypes *Cast_COI*_7, 8, 9, 10, 11 and 13 only in *C. ambigua*, and haplotypes *Cast_COI*_3, 5, 6, 7, 11, and 12 in both taxa or in their "*C. ambigua*-like" individuals. The *C. inflata* haplotypes tended toward the middle of the haplotype network, *C. ambigua* haplotypes to the edges, and those of "*C. ambigua*-like" individuals from the center to the right.

At the mitochondrial *16S rRNA* region, 70 samples from the Rio Paraguay watershed were sequenced (19 of *C. ambigua*, 43 of *C. inflata*, and 8 of *C. ambigua*-like). We also considered variation among *C. ambigua* from the Amazon River watershed [20] as a geographical outgroup. Within a 443-bp sequence, 38 variable nucleotides defined 9 haplotypes in the Rio Paraguay and 7 in the Amazon River watersheds (Table 6), which have been reported as the GenBank accession numbers indicated at the right margin of the table. Our *16S rRNA* sequences were 93–94% similar to the *C. duprei* and 96% similar to the *C. quadrata* reference sequences retrieved from GenBank. Metrics of genetic variation at the mitochondrial *16S rRNA* region (Table 7) were lower than those for the *COI* region. Metrics for *C. inflata* were generally higher than for *C. ambigua* and were higher for *C. inflata* in the lowlands (Valo Verde Lake, Claro Stream) than at the edge of their distribution in the highlands (Baixo Stream).

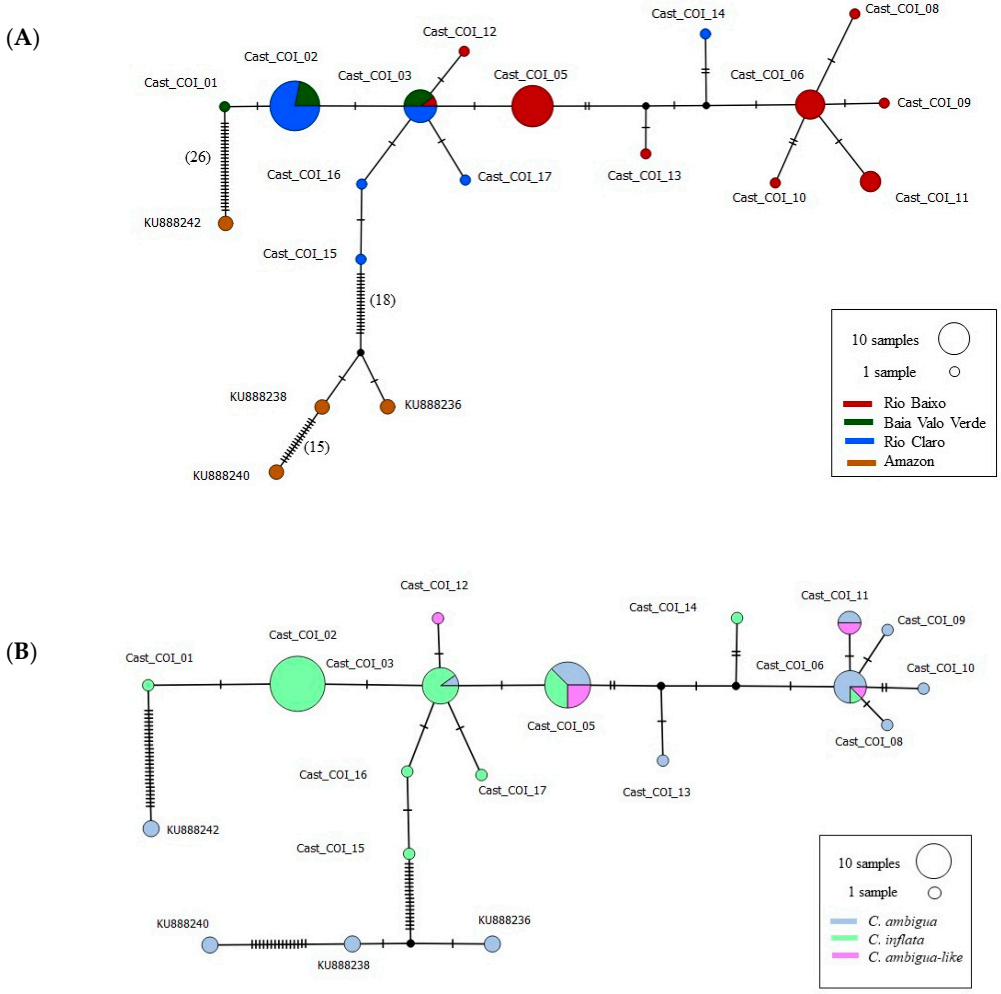

Figure 5. Haplotype networks for mitochondrial *COI* for *C. ambigua* and *C. inflata* across the Paraguay and Amazon River basins, considered: (**A**). on a geographic basis, and (**B**). on a taxonomic basis. The relative sizes of the circles reflect the frequencies of the respective haplotypes. Hash marks indicate the number of inferred mutations among haplotypes observed. Black dots represent inferred intermediate haplotypes that were not observed in our data set. Haplotype designations include *Cast* for *Castalia*, *COI* for cytochrome oxidase, and a number for each unique DNA sequence.

Table 6. Haplotypes for *Castalia* species at the mitochondrial *16S rRNA* gene. Haplotypes *Cast_16S*_01 through 9 are original data for samples from the upper Paraguay River basin; *C. ambigua* 1 through 7 are from samples from the upper Amazon River basin [20]. Numbers refer to nucleotide position.

	35	**36**	**83**	**87**	**92**	**98**	**111**	**119**	**124**	**125**	**138**	**149**	**176**	**184**	**186**	**191**	**197**	**200**	**206**	**211**	**214**	**217**	**246**	**258**	**262**	**263**
Cast 16S 1	A	A	C	T	C	A	C	C	C	C	G	C	G	T	A	T	T	T	A	C	T	A	T	T	C	C
Cast 16S 2	.	.	.	.	.	.	.	.	.	.	.	.	.	.	.	.	.	.	.	.	.	.	.	.	.	.
Cast 16S 3	.	.	.	.	.	.	.	.	.	.	.	.	A	.	.	.	.	.	.	.	.	.	.	.	.	.
Cast 16S 4	.	.	.	.	.	.	.	.	.	.	.	.	.	.	.	.	.	.	.	.	.	.	.	.	.	.
Cast 16S 5	.	.	.	.	.	.	.	.	.	.	.	.	.	.	G	.	.	.	.	.	.	.	.	.	.	.
Cast 16S 6	.	.	.	.	.	.	.	.	.	.	.	.	.	.	.	.	.	.	.	.	.	.	.	.	T	.
Cast 16S 7	.	.	T	.	.	.	.	.	.	.	.	.	.	.	.	.	.	.	.	.	.	.	.	.	.	.
Cast 16S 8	.	.	.	.	.	.	.	.	.	.	.	.	.	.	.	.	.	.	.	.	.	.	.	.	.	.
Cast 16S 9	.	.	.	.	.	.	.	.	.	.	.	.	.	.	.	C	.	.	.	.	.	.	.	.	.	.
C. ambigua 1	C	T	.	.	.	.	.	T	.	.	.	T	.	C	.	.	C	.	C	.	C	.	.	.	T	.
C. ambigua 2	T	.	.	.	.	.	.	T	.	.	.	T	.	C	.	.	C	.	C	.	C	.	.	.	T	.
C. ambigua 3	.	.	.	.	.	.	.	T	.	.	.	T	.	C	.	.	C	C	C	.	C	.	.	.	T	.
C. ambigua 4	.	.	.	.	.	.	.	T	.	T	.	T	.	C	.	.	C	.	C	.	C	.	.	.	T	.
C. ambigua 5	T	.	.	.	.	.	.	T	.	.	.	T	.	.	.	.	C	.	.	T	.	.	.	.	T	.
C. ambigua 6	C	.	.	.	.	.	.	T	.	.	.	T	.	.	.	.	C	.	.	T	.	.	.	.	T	.
C. ambigua 7	T	T	.	C	A	G	T	.	T	.	A	T	.	C	.	.	C	.	.	.	C	G	C	C	A	T

	265	**269**	**273**	**276**	**280**	**291**	**292**	**336**	**390**	**400**	**413**	**428**	***C. ambigua***	***C. inflata***	***C. ambigua*-like**	**Rio Baixo**	**Baia Valo Verde**	**Rio Claro**	**Rio Amazonas**	**Accession number**
Cast 16S 1	A	G	T	C	T	T	G	C	C	T	T	G		7			6	1		KY463457
Cast 16S 2	.	.	.	.	.	.	.	.	.	C	.	.	18	30	7	32	3	20		KY463458
Cast 16S 3	.	.	.	.	.	.	.	T	T	C	.	.		1			1			KY463459
Cast 16S 4	.	.	.	.	.	.	.	.	.	C	.	T	1			1				KY463460
Cast 16S 5	.	.	.	.	.	.	.	.	.	C	.	.			1	1				KY463461
Cast 16S 6	.	.	.	.	.	.	.	.	.	C	C	.		2				2		KY463462
Cast 16S 7	.	.	.	.	.	.	.	T	.	C	.	.		1				1		KY463463
Cast 16S 8	.	.	.	.	.	.	A	.	.	C	.	.		1				1		KY463464
Cast 16S 9	.	.	.	.	.	.	.	.	.	C	.	.		1				1		KY463465
C. ambigua 1	C	.	.	A	C	C	.	A	-	-	-	-	1						1	KU888207
C. ambigua 2	C	.	.	A	C	C	.	A	-	-	-	-	1						1	KU888208
C. ambigua 3	C	.	.	A	C	C	.	T	-	-	-	-	1						1	KU888209
C. ambigua 4	C	.	.	A	C	C	.	T	-	-	-	-	1						1	KU888210
C. ambigua 5	C	.	C	A	C	.	.	A	-	-	-	-	1						1	KU888211
C. ambigua 6	C	.	C	A	C	.	.	A	-	-	-	-	1						1	KU888212
C. ambigua 7	C	A	C	T	C	C	.	A	-	-	-	-	1						1	KU888213

Table 7. Variation at the mitochondrial *16S* region for *Castalia* species among three sites in the upper Paraguay River basin (original data) and the upper Amazon River basin of Brazil [20].

Species	Collection Area	*n*	Number of Haplotypes	Average Number of Nucleotide Differences (*k*)	Haplotype Diversity (*h*)	Nucleotide Diversity (π)
C. ambigua	Baixo Stream	19	2	0.105	0.105	0.0002
C. inflata	Baixo Stream	7	1	0.000	0.000	0.0000
C. ambigua-like	Baixo Stream	8	2	0.250	0.250	0.0006
C. inflata	Valo Verde Lake	10	3	1.133	0.600	0.0026
C. inflata	Claro Stream	26	6	0.680	0.412	0.0015
C. ambigua	Amazon River	7	7	9.333	1.000	0.0308

Because the *16S rRNA* sequences from da Cruz Santos-Neto et al. [20] are shorter than ours, after trimming ours to equal length, some of our haplotypes became the same. Identical sequences after trimming were *Cast_16S*_01, *Cast_COI*_02, and *Cast_16S*_04. All geographic sites within the Rio Paraguay basin exhibited multiple *16S* rRNA haplotypes (Figure 6A), with the respective populations showing different haplotype frequencies. Haplotype frequencies differed across nominal taxa (Figure 6B). Most *C. inflata* individuals exhibited haplotype *Cast_16S*_2, with some individuals showing any of six haplotypes no more than three mutational steps from *Cast_16S*_2. Most *C. ambigua* individuals exhibited the *Cast_16S*_2 haplotype, with one individual showing the closely related *Cast_16S*_4. The *C. ambigua*-like individuals exhibited the common *Cast_16S*_2 haplotype and one closely related *Cast_16S*_5. Notably, all Amazon River haplotypes were at least 12 mutational steps removed from all Rio Paraguay haplotypes. On a taxonomic basis (Figure 6B), most *C. inflata* and *C. ambigua*-like haplotypes were among the *C. ambigua* haplotypes.

A 559-bp segment of the internal transcribed spacer (*ITS1*) of the nuclear *18S rRNA* gene was sequenced in 46 individuals, including seven *C. ambigua*, 36 *C. inflata*, and three *C. ambigua*-like individuals. The use of software packages Clustal and Webprank resulted in the same alignment of our sequences. No variable nucleotides were observed. The sequence is reported as GenBank accession number KY463466. Gaps resulted when our *Castalia 18S rRNA* sequences were aligned with those of outgroup *Callonaia duprei* (KU888175), and four indels were coded using FastGap v1.2.

A total of 75 samples were sequenced at the nuclear *28S* rRNA gene: 10 *C. inflata* from Valo Verde Lake, 27 *C. inflata* from Claro Stream, and 38 *C. inflata*, *C. ambigua*, and "*C. ambigua*-like" from Baixo Stream. One haplotype was observed across 441 nucleotides among all individuals and is reported as GenBank accession number KT885158.

A 354-bp segment of the histone *H3NR* gene was sequenced among 64 individuals, 19 *C. ambigua*, 37 *C. inflata*, and eight *C. ambigua*-like. The same nucleotide sequence was observed among all individuals and is reported as GenBank accession number KY474373.

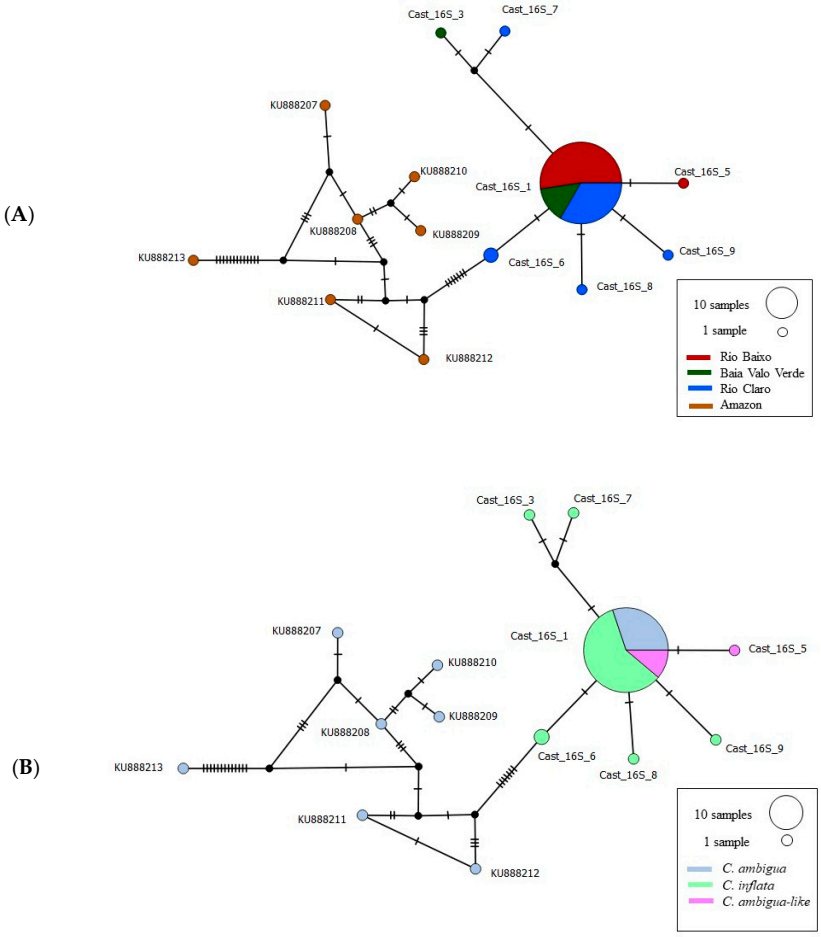

Figure 6. Haplotype networks for mitochondrial *16S rRNA* for *Castalia ambigua* and *C. inflata* across the Paraguay and Amazon River basins, considered: (**A**). on a geographic basis, and (**B**). on a taxonomic basis. The relative sizes of the circles reflect the frequencies of the respective haplotypes. Hash marks indicate the number of inferred mutations among haplotypes observed. Black dots represent inferred intermediate haplotypes that were not observed in our data set. Haplotype designations include *Cast* for *Castalia*, *16S* for *16S rRNA*, and a number for each unique DNA sequence.

For phylogenetic analysis of the *COI* sequence data set, the General Time Reversible (GTR) with invariable sites model was selected. For *16S* sequences, the General Time Reversible (GTR) model with gamma distribution and a proportion of invariable sites [65] was selected as the most appropriate evolutionary model. For *18S ITS1*, the GTR model with equal rates was found to be the most suitable. For the combined *COI* + *16S* sequences, the most appropriate evolutionary model was the Hasegawa–Kishino–Yano (HKY) with gamma distribution and a proportion of invariable sites [61]. Phylogenetic trees constructed using Bayesian analysis, which we discuss below, showed the inferred evolutionary relationships of mussel populations that we sampled within the larger context of regional variation. Phylogenetic trees constructed using maximum likelihood (not shown) yielded trees with topologies that were virtually the same as those from the Bayesian analysis.

The phylogenetic tree showing relationships among mitochondrial *COI* haplotypes (Figure 7) exhibited both geographic and phylogenetic patterns. The two lower clusters included haplotypes from *C. ambigua* from the Amazon River basin observed by da Cruz Santos-Neto et al. [20] and are shown in brown. The large upper cluster was comprised of all of our samples from the Paraguay River basin, a cluster including a mixture of haplotypes from nominal *C. ambigua*, *C. inflata*, and *C. ambigua*-like individuals from all three geographic sites.

Phylogenetic analysis of mitochondrial *16S rRNA* sequence haplotypes (Figure 8) clearly separated haplotypes of *C. ambigua* and *C. inflata* from those of outgroup *Triplodon corrugatus* (Lamarck, 1819). Haplotypes of *C. ambigua* from the Amazon River were clearly separated from those of all nominal *Castalia* species from the Paraguay drainage.

Phylogenetic analyses of combined mitochondrial *COI* and *16S* sequences (Figure 9) showed stronger evidence of geographic than of nominal species structure. At the most basal node in the tree, the combined haplotype of the outgroup *T. corrugatus* sequence was basal to all others. The second node separated haplotypes of *C. ambigua* from the Amazon basin from all those of all nominal species from the Paraguay basin.

Phylogenetic analysis of our one observed *ITS1* haplotype, those of *C. ambigua* from the Amazon basin [20] and outgroups *C. stevensi* (H.B. Baker, 1930) and *Callonaia duprei* (Figure 10) showed clear distinction of *Castalia* haplotypes from those of *Callonaia*. All *Castalia* haplotypes clustered tightly together.

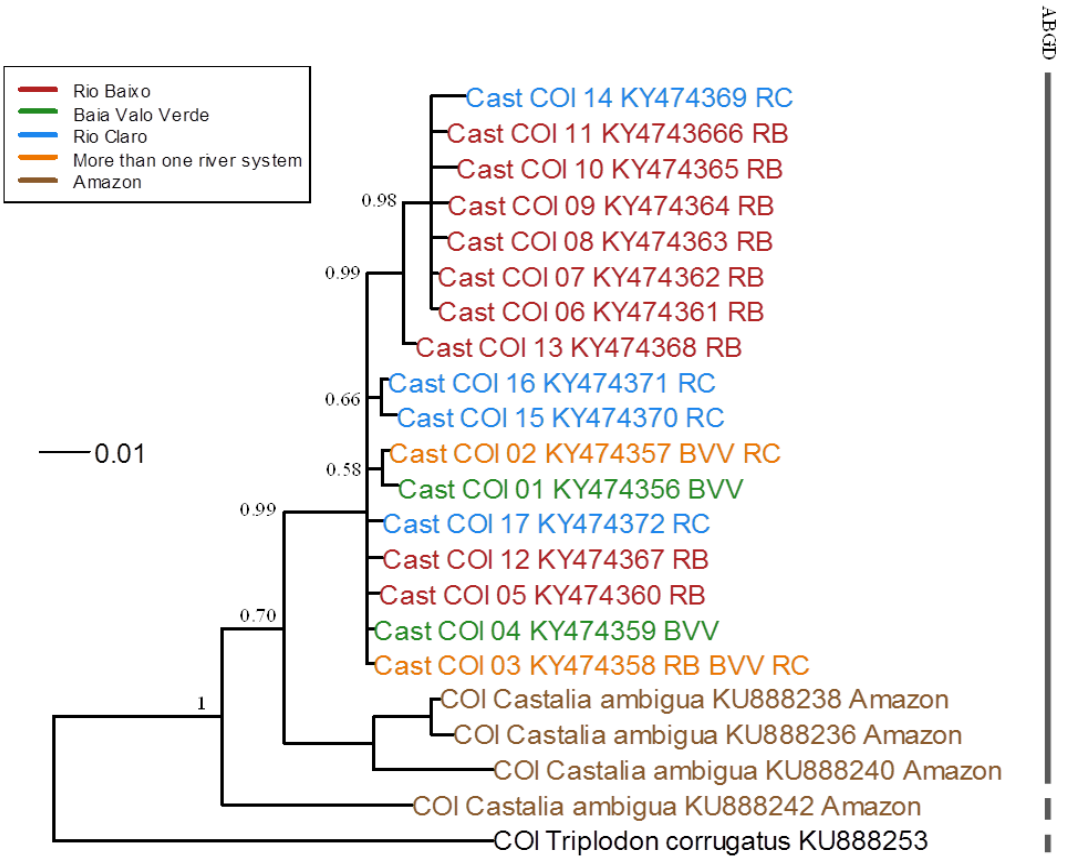

Figure 7. Bayesian phylogenetic analysis showing the relationships among the *COI* sequence haplotypes (KY474356–KY474372) and other 4 sequences for *C. ambigua* (KU888238, KU888236, KU888240, and KU888242) obtained from Genbank. The outgroup was *Triplodon corrugatus* (KU888253). The alignment of these sequences resulted in 454-bp DNA sequence. The analysis was run for 600,000 generations to create a set of trees, of which 9002 were sampled. The Bayesian phylogenetic consensus tree had a final average standard deviation of split frequencies of 0.006727 and with a −ln likelihood of −1212.66 Branch lengths are proportional to inferred evolutionary distances. Numerals to the left of nodes indicate posterior probability support for the respective nodes. Designators for each DNA sequence include the location (RC—Claro Stream, BVV—Vale Verde Lake, RB—Baixo Stream). The distance bar is shown in units of substitutions per nucleotide site. ABGD on the right margin refers to species delimitations suggested by Automatic Barcode Gap Discovery [57].

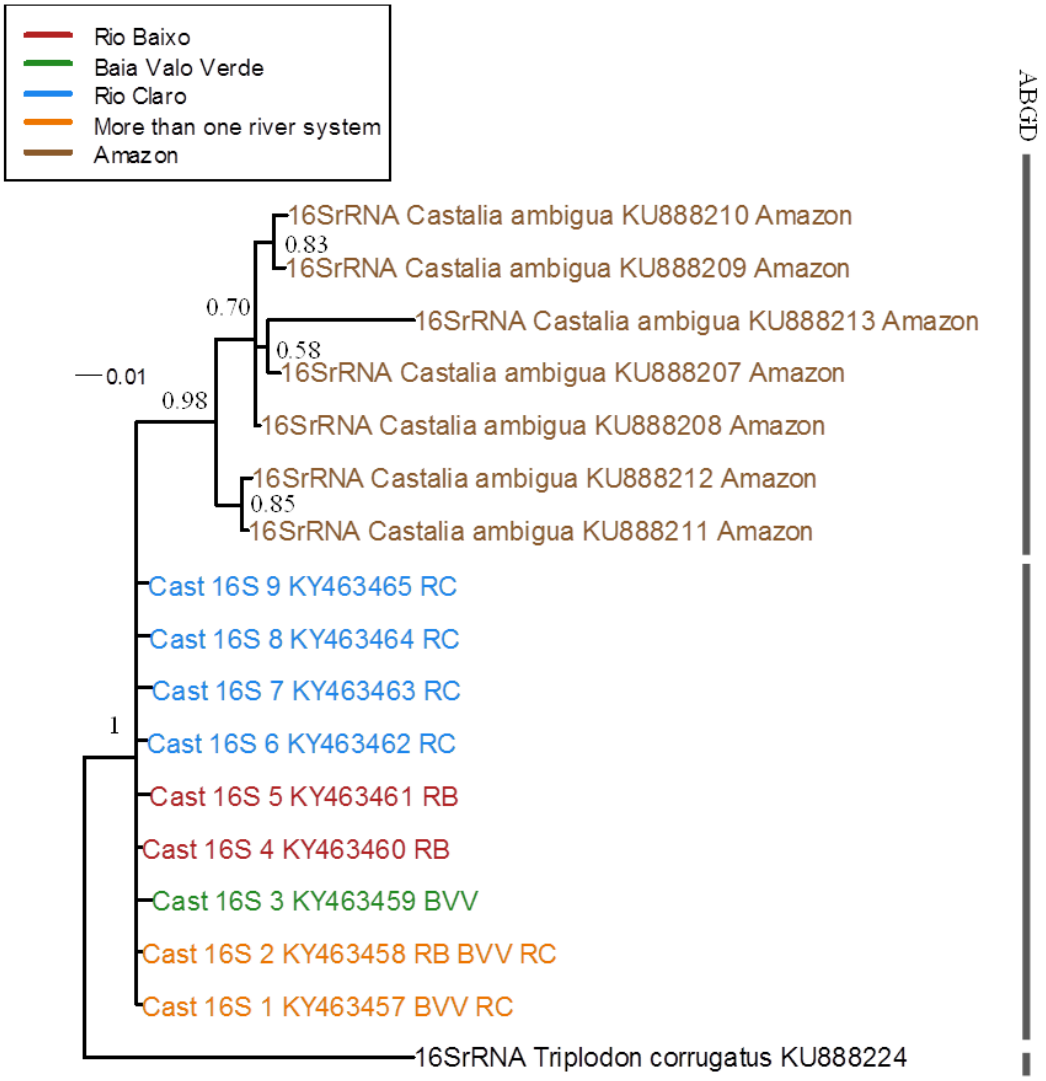

Figure 8. Bayesian phylogenetic analysis showing the relationships among the *16S rRNA* haplotypes. In addition, seven individuals of *C. ambigua* (KU888207–KU888213) that were obtained from GenBank were included. The alignment of these sequences resulted in 308bp sequences. The analysis was run with a total of 500,000 generations, the final average standard deviation of split frequencies was 0.004356 with a −ln likelihood of −822.58. a total of 7501 trees were sampled. Branch lengths are proportional to inferred evolutionary distances. Numerals to the left of nodes indicate posterior probability support for the respective nodes. Designators for each DNA sequence include the location (RC—Claro Stream, BVV—Vale Verde Lake, RB—Baixo Stream). The distance bar is shown in units of substitutions per nucleotide site. ABGD on the right margin refers to species delimitations suggested by Automatic Barcode Gap Discovery [57].

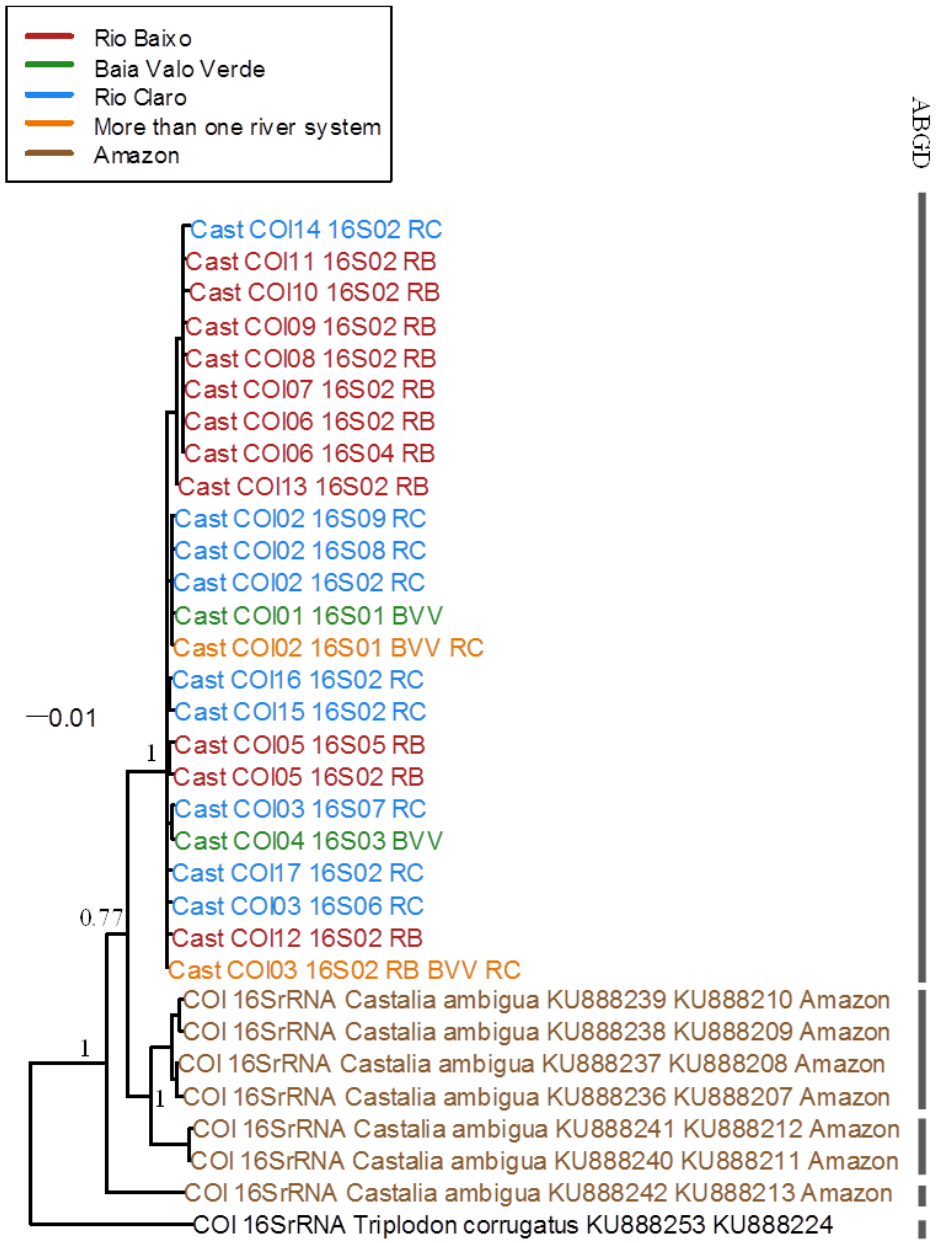

Figure 9. Bayesian phylogenetic analysis showing the relationships among individual mussels inferred from the combined mitochondrial *COI* and *16S rRNA* DNA sequences (762 base-pairs) for *C. ambigua*, *C. ambigua*-like, *C. inflata*, and outgroup reference sequence for *Triplodon corrugatus* (KU888253). The analysis was run for 1.5 million generations to create a set of trees, of which 22,502 were sampled. The Bayesian phylogenetic consensus tree had a final average standard deviation of split frequencies of 0.002664 and with a −ln likelihood of −2122.95. Branch lengths are proportional to inferred evolutionary distances. Numerals to the left of nodes indicate posterior probability support for the respective nodes. Designators for each DNA sequence include the location (RC—Claro Stream, BVV—Vale Verde Lake, RB—Baixo Stream). The distance bar is shown in units of substitutions per nucleotide site. ABGD on the right margin refers to species delimitations suggested by Automatic Barcode Gap Discovery [57].

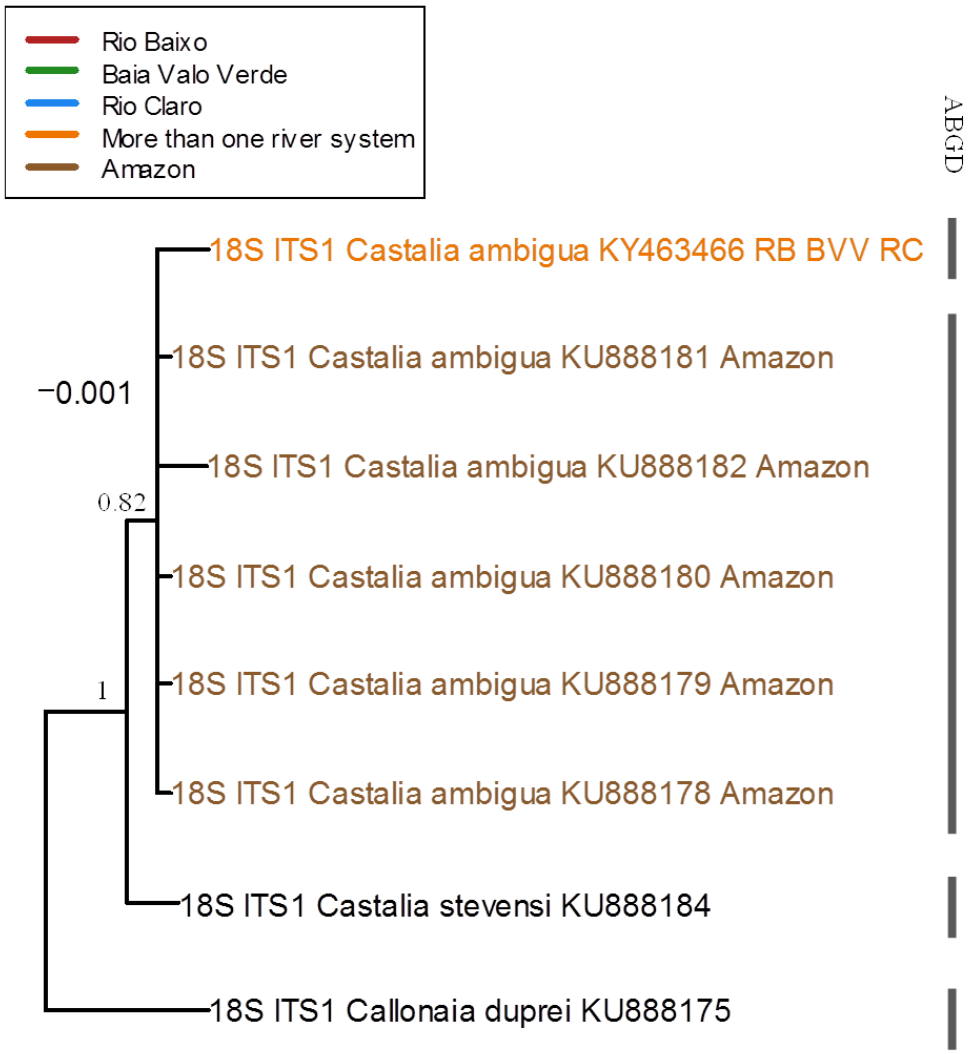

Figure 10. Bayesian phylogenic analysis showing the relationships among our one *18S ITS* haplotype sequence (KY463466) and other sequences for *Castalia ambigua* (KU888178, KU888179, KU888180, KU888182, and KU888181) obtained from Genbank. The outgroups were *Castalia stevensi* (KU888184) and *Callonaia duprei* (KU888175). The alignment of these sequences resulted in 515bp sequences. The analysis was run for 500,000 generations to create a set of trees, of which 2178 were sampled. The Bayesian phylogenetic consensus tree had a final average standard deviation of split frequencies of 0.005394 and with a −ln likelihood of −846.10. Branch lengths are proportional to inferred evolutionary distances. Numerals to the left of nodes indicate posterior probability support for the respective nodes. The distance bar is shown in units of substitutions per nucleotide site. ABGD on the right margin refers to species delimitations suggested by Automatic Barcode Gap Discovery [57].

3.4. Historical Demography

Scenario 2 (where populations in the Paraguay and Amazon basins differentiated before the three populations within the Paraguay basin did) was identified as the most highly supported demographic scenario by our DIYABC analysis, with a posterior probability of 0.994 (0.993–0.995), compared to Scenario 1 (all four populations diverged at the same time from a common ancestor with equal divergence rates) with a posterior probability of 0.006 (0.005–0.007). The Type I and II error rates for Scenario 2 were both <1%, which are very low, and thus when combined with the much higher posterior probability suggests that Scenario 2 is the best-supported scenario to explain the data. For Scenario 2, the median posterior distributions of N_e ranged from a high of ~32,600 for the Amazon

River population to a low of ~4020 for the Valo Verde Lake population, median divergence times of populations at t_1 was ~1290 generations ago (~7095 years ago) and at t_2 it was ~7240 generations ago (~39,820 year ago), and the median mutation rate was 6.64×10^{-7} (Table 3).

4. Discussion

4.1. Distribution, Morphology, and Taxonomy

Due to the high number of species in the genus *Castalia* Lamarck (1819)—thirteen [8,66] to seventeen [3] in total—and their widespread occurrence throughout South America, the literature on distribution and identification of some member species, such as *C. ambigua* and *C. inflata*, remains confusing, with many records of occurrence uncertain [10,11] (Figure 1A). Records for *C. inflata* have always been common in mid-southern South America, where the type locality was described from specimens collected in the Parana River, in the province of Corrientes in Argentina. The initial records were from the lower Paraná River (von Ihering, cited in 10); small tributaries of the Paraná River (D'Orbigny) in Argentina, to the Paraguay River near the Apa River in Mato Grosso do Sul and upstream at Cáceres in Mato Grosso, both in Brazil (von Ihering, cited in 10). Recently, this species was recorded in the Paraná River in Santa Fé, Argentina [5,31]; in the La Plata River in Uruguay [11]; and at the confluence of the Apa and Paraguay rivers in Paraguay [19]. In Brazil, *C. inflata* was reported in the Bento Gomes River at Poconé in Mato Grosso [23,32,67], the Uruguay River at Uruguaiana in Rio Grande do Sul [33], and associated with several reaches and marginal lakes of the Cuiabá River in the Pantanal in Mato Grosso [22,34].

The occurrence of *C. ambigua* is better documented; the description of the type specimen is from the Amazon Basin, but there are records in other major watersheds of South America, occurring from the Magdalena River basin in Colombia to the La Plata River in Argentina [11] and the San-Miguel and Guarayos rivers in Bolivia [9]. In Brazil, this species occurs at the confluence of the Rio Negro with the Solimões River [36]; the Uraricoera and Branco River [68]; the Aripuanã River [37], Tocantins River [35]; and the Irituia River [6] in the Amazon; in the Cuiabazinho River in Mato Grosso [64], and there are records for the São Francisco River basin [11].

The distributions of the nominal taxa *C. ambigua* and *C. inflata* meet at the northern portion of the upper Paraguay River basin. In our study system, *C. ambigua* occurred exclusively in lotic waters with relatively high primary productivity and high conductivity (230–370 $\mu S/cm^3$). Such environments occur only in the highlands, in the headwaters region of the upper basin associated with streams and rivers rich in calcium derived from calcareous springs. On the other hand, the distribution of *C. inflata* was linked to lowlands in silted environments, fine substrates, high concentrations of particulate organic matter, and low conductivity (35 to 70 $\mu S/cm^3$), commonly in wetlands under the influence of the flood pulse, as in the Pantanal. Recent studies carried out on rivers in the Amazon hydrographic basin have shown that the shape of the shell in the Hyriini is largely associated with drainage characteristics [69].

Our morphometric data showed a variation of biometric characters (length, width, and height) from each nominal species. However, some points overlapped, reflecting a phenotypic gradient. In the upper Paraguay basin, there have been reports of the occurrence of two distinct species identified as *C. ambigua* and *C. inflata* using only conchological traits [64]. However, visual differentiation is not always effective because the shell shape is subject to marked phenotypic plasticity [25,70].

4.2. Molecular and Phylogenetic Analyses

Our field collections of *Castalia* species in the upper Paraguay basin revealed individuals in Baixo Stream in the uplands whose appearance was intermediate between the classical morphologies of *C. ambigua* and *C. inflata*. Hence, we screened genetic markers to characterize their molecular genetic and phylogenetic affinities. Genetic identification of tropical freshwater mussels has been approached through the amplification and sequencing of the cytochrome oxidase I (*COI*) gene of mitochondrial DNA and the *28S* nuclear rDNA gene [71]. Because few genetic markers have been established for

tropical freshwater mussels, we screened variation at three additional genes (mitochondrial *16S rRNA*, nuclear *18S rRNA-ITS*, and histone *H3*) that are sufficiently well conserved across a range of taxa that primers proving useful for PCR amplification are available.

Our morphological and mitochondrial results supported neither reproductive isolation nor reciprocal monophyly among *C. ambigua* and *C. inflata* at the upland Baixo Stream site. To explain the results, we note the occurrence of shell plasticity in unionids; the tendency for shell morphology to vary from compressed in headwaters to inflated downstream, sometimes with tubercles, has been noted in many freshwater mussel species. Reviewing the literature of his time, Ortmann [25] noted numerous examples in his own and colleagues' work. Subsequent work [reviewed by Reference 70] showed this ecotypic pattern within the tribes Pleurobemeni (genera *Fusconaia*, *Pleurobema*, and *Pleuronaia*), Quadrulini (*Cyclonaias*, *Quadrula*), Lampsilini (*Actinainais ligamentina*, *Epioblasma torulosa*, *Dromus*, and *Obovaria*), and Amblemini (*Ambema plicata*). Using 103 amplified fragment length polymorphism (AFLP) markers, Zieritz et al. [72] showed that morphological differences in shell morphology in *Unio pictorum* were the result of phenotypic plasticity, and did not reflect genetic differentiation. Shell convexity in the freshwater pearl mussel *Margaretifera margaretifera* may be affected by thermal effects [73], suggesting that the thermal regimes in colder upland and warmer lowland sites could have affected the morphologies of mussel populations that we studied. Failure to account for shell plasticity in unionoids has resulted in the description of species or subspecies that are not supported by molecular phylogenetic analyses. Inoue et al. [74] showed that morphological differences between *Obovaria jacksoniana* and *Villosa arkansasensis* were due to ecophenotypic plasticity and suggested that these species were synonymous. Morphological plasticity is such that the four recognized *Unio* species in France actually include three or five valid species [75]. Our results suggest that *Castalia ambigua* and *C. inflata* within the upper Paraguay River drainage are not phylogenetically distinct, constituting a case of ecotypic variation within one lineage. Further testing of the hypothesis that these nominal species are valid would require analysis of populations across the geographic extent of the ranges of the nominal species.

Analyses of our DNA sequencing results for mitochondrial *COI*, *16s rRNA*, and combined sequences showed phylogenetic differentiation among *C. ambigua* from the Paraguay and Amazon basins. We interpret the shared ancestry and subsequent differentiation as a consequence of the geological history of the region. Prior to the Miocene, a paleo-Amazon-Orinoco drainage originating in Chile and Argentina drained northward to the Caribbean Sea. The modern watershed divide between the Paraguay and Amazon systems arose approximately 30 million years ago with the initiation of tectonic activity, driving the diversification not only of fishes [76] but presumably also freshwater mussels.

4.3. Conclusions and Prospects

After examining phenotypic and genetic variation in *Castalia ambigua* and *C. inflata* in the upper Paraguay River basin, the results of our phylogenetic analyses are most consistent with the hypothesis of nominal species belonging to one evolutionary lineage. The phenotypic variation that we observed in the upper Paraguay system is consistent with the tendency of shell morphologies to vary from headwaters to lowland areas, which has long been recognized in North American freshwater mussels and may also apply to South American mussels. Supporting this interpretation, we noted a strong phylogenetic distinction among *C. ambigua* between the Paraguay and Amazon basins, which may be indicative of species-based differences. Broad-scale phylogeographic examination including examination of type specimens will inform defensible delineation of *Castalia* species and members of other lineages within the South American freshwater mussel fauna.

Author Contributions: Conceptualization, C.C. and E.H.; methodology, C.C., E.H., and J.J.; software, M.O.-H. and J.J.; validation, C.C., M.C.M., E.H., and J.J.; formal analysis, M.O.-H. and J.J.; investigation, E.H., M.O.-H., B.V.; resources, R.S., G.d.C.S.N., M.C.M. and P.M.; writing—review and editing, M.O.-H., E.H., R.S., J.J., G.d.C.S.N., M.C.M., and C.C.; visualization, M.O.-H., J.J., G.d.C.S.N.; supervision, C.C. and E.H.; project administration,

E.H. and C.C.; funding acquisition, C.C. and E.H. All authors have read and agreed to the published version of the manuscript.

Funding: This research was supported by the Universidade Federal de Mato Grosso, Pro Reitoria de Pesquisa, CNPq Process number 400357/2014-3, PVE/CNPq Process no. 400357/2014-3, FAPEMAT Process no. 751046/2011, and 2011 and SECRI/UFMT Apoio a Pesquisador Visitante Internacional 2014.

Acknowledgments: The authors would like to thank Aruã Callil for shell pictures and Vinicius C. Costa Soares for laboratory support. Murray Hyde assisted in the molecular genetics laboratory and data analysis.

Conflicts of Interest: The authors declare no conflict of interest.

References

1. Mansur, M.C.D.; Pereira, D.; Bergonci, P.E.A.; Pimpão, D.M.; Barradas, J.R.S.; Sabaj, M.H. Morphological assessment of *Rheodreissena* (Bivalvia: Veneroida: Dreissenidae) with an updated diagnosis of the genus, descriptions of two new species, redescription of *R. lopesi*, and the first account of larval brooding in New World dreissenids. *Proc. Acad. Nat. Sci. Phila.* **2019**, *166*, 1–45. [CrossRef]
2. Jaeckel, S.G.A. Die mollusken Sudamerikas. In *Biogeography and Ecology in South America*; Fittkau, E.J., Illiea, J., Klinge, H., Schwabe, G.H., Sioli, H., Eds.; Dr. W. Junk n. v. Publishers: The Hague, The Netherlands, 1969; Volume 2, pp. 794–827.
3. Pereira, D.; Mansur, M.C.D.; Duarte, L.D.S.; de Oliveira, A.S.; Pimpao, D.M.; Callil, C.T.; Ituarte, C.; Parada, E.; Peredo, S.; Darrigan, G.; et al. Bivalve distribution in hydrographic regions in South America: Historical overview and conservation. *Hydrobiologia* **2014**, *735*, 15–44. [CrossRef]
4. Torres, S.; Cao, L.; Gregoric, D.E.G.; de Lucía, M.; Brea, F.; Darrigran, G. Distribution of the Unionida (Bivalvia, Paleoheterodonta) from Argentina and its conservation in the southern Neotropical region. *PLoS ONE* **2018**, *13*, e0203616. [CrossRef] [PubMed]
5. Bonetto, A.A. *Notas Sobre los Generos Castalina y Castalia en el Paraná Médio e Inferior*; Direccion General de Recursos Naturales, Ministerio de Agricultura e Ganaderia: Santa Fé, Brazil, 1961.
6. Vale, R.S.; Beasley, C.R.; Tagliaro, C.H.; Mansur, M.C.D. The glochidium and marsupium of *Castalia ambigua ambigua* Lamarck, 1819, from northern Brazil. *Am. Malacol. Bull.* **2005**, *20*, 43–48.
7. Mansur, M.C.D. Lista dos Moluscos bivalves das famílias Hyriidae e Mycetopodidae para o estado do Rio Grande do Sul. *Iheringia Série Zool.* **1970**, *39*, 33–95.
8. Graf, D.L.; Cummings, K.S. MUSSELp: The Mussel Project Website. 2015. Available online: http://mussel-project.uwsp.edu/ (accessed on 9 October 2018).
9. D'Orbigny, A. *Voyage dans L'Amerique Méridionale. Tome Cinquéme, 3ª Partie: Molusques*; P Bertrand: Paris, France, 1843.
10. Ortmann, A.E. South American naiads: A contribution to the knowledge of the freshwater mussels of South America. *Mem. Carnegie Mus.* **1921**, *8*, 415–670.
11. Bonetto, A.A. Las almejas sudamericanas de la Tribu Castaliini. *Physis* **1965**, *25*, 187–196.
12. Rumi, A.; Gregoric, D.E.G.; Nunez, V.; Darrigan, G.A. Malacología Latinoamericana: Moluscos de agua dulce de Argentina. *Rev. Biol. Trop.* **2008**, *56*, 77–111. [CrossRef]
13. Figueiras, A. La malacofauna dulceacuícola del Uruguay (Parte II). *Commun. Soc. Malacol. Urug.* **1965**, *1*, 223–270.
14. Schade, F.H. Lista de los moluscos del Guaira (Villarrica—Paraguay) conocidos hasta el presente. *Commun. Soc. Malacol. Urug.* **1965**, *1*, 209–221.
15. Simone, L.R.L. *Land and Freshwater Molluscs of Brazil: An Illustrated Inventory of the Brazilian Malacofauna, Including Neighboring Regions of South America, Respect to the Terrestrial and Freshwater Ecosystems*; FAPESP (Sao Paulo Research Foundation): Sao Paulo, Brazil, 2006.
16. Graf, D.L.; Cummings, K.S. Review of the systematics and global diversity of freshwater mussel species (Bivalvia: Unionoida). *J. Molluscan Stud.* **2007**, *73*, 291–314. [CrossRef]
17. Bogan, A.E. Mollusca-Bivalvia Checklist. Freshwater Animal Biodiversity Project. 2010. Available online: http://fada.biodiversity.be/CheckLists/Mollusca-Bivalvia.pdf (accessed on 9 October 2018).
18. Haas, F. Superfamilia Unionacea. *Das Tierreich* **1969**, *88*, 1–663.
19. Quintana, M.G. Catologo preliminar de la malacofauna del Paraguay. *Rev. Mus. Argent. Cienc. Nat. Bernardino Rivadavia Cienc. Zool.* **1982**, *11*, 61–158.

20. Da Cruz Santos-Neto, G.; Beasley, C.R.; Schneider, H.; Pimpao, D.M.; Hoeh, W.R.; De Simone, L.R.L.; Tagliaro, C.H. Genetic relationships among freshwater mussel species from fifteen Amazonian rivers and inferences on the evolution of the Hyriidae (Mollusca: Bivalvia: Unionida). *Mol. Phylogenet. Evol.* **2016**, *100*, 148–159. [CrossRef]
21. Ministerio de Agricultura y Ganaderia. *Fauna Amenazada del Paraguay*; Direccion de Parques Nacionales y Vida Silvestre, Fundacion Moises Bertoni: Asuncion, Paraguay, 1998.
22. Colle, A.C.; Callil, C.T. Environmental influences on the composition and structure of the freshwater mussels in shallow lakes in the Cuiabá River floodplain. *Braz. J. Biol.* **2012**, *72*, 249–256. [CrossRef]
23. Santos, R.C.L.; Callil, C.T.; Landeiro, V.L. Unraveling the effects of water–sediment conditions and spatial patterns on Unionida assemblages in seasonally connected floodplain lakes. *Hydrobiologia* **2020**, *847*, 2909–2922. [CrossRef]
24. Junk, W.J.; Piedade, M.T.F.; Candotti, E. Água no Brasil: Excesso, escassez e problemas crescentes. *Ciência Hoje* **2014**, *53*, 52–53.
25. Ortmann, A.E. Correlation of shape and station in fresh-water mussels (naiades). *Proc. Am. Phil. Soc.* **1920**, *59*, 268–312.
26. Varis, O.; Tortajada, C.; Biswas, A.K. *Management of Transboundary Rivers and Lakes*; Springer: Berlin/Heidelberg, Germany, 2008; p. 271.
27. Gotelli, N.; Ellison, A.M. *Princípios de Estatística em Ecologia*; Artmed: Porto Alegre, Brazil, 2010; 683p.
28. R Core Team. *R: A Language and Environment for Statistical Computing*; R Foundation for Statistical Computing: Vienna, Austria, 2018; Available online: https://www.R-project.org (accessed on 28 November 2018).
29. Tang, Y.; Horikoshi, M.; Li, W. Ggfortify: Unified interface to visualize statistical result of popular R packages. *R J.* **2016**, *8*, 478–489. [CrossRef]
30. Naimo, T.S.; Damschen, E.D.; Rada, R.G.; Monroe, E.M. Nonlethal evaluations of the physiological health of unionid mussels: Methods for biopsy and glycogen analysis. *J. N. Am. Bentholog. Soc.* **1998**, *17*, 121–128. [CrossRef]
31. Bonetto, A.A. *Algunos Factores Ecologicos Vinculados a la Distribucion Geografica de las Nayades em el Rio Paraná y sus Afluentes*; Dirección General de Recursos Naturales, Ministerio de Agricultura e Ganaderia: Santa Fé, Brazil, 1962.
32. Serrano, M.A.; Tietbothl, R.S.; Mansur, M.C.D. Sobre a ocorrência de moluscos bivalvia no Pantanal de Mato Grosso, Brasil. *Biociências* **1998**, *6*, 131–144.
33. Castillo, A.R.; Brasil, L.G.; Mansur, M.C.D.; Querol, E.; Querol, M.V.M.; Olivera, E.V. Moluscos bivalves da localidade de São Marcos, bacia do Médio rio Uruguai, Uruguaiana, Brasil. *Biotemas* **2007**, *20*, 73–79.
34. Wantzen, K.M.; Callil, C.T.; Butakka, C.M.M. Benthic invertebrates of the Pantanal and its tributaries. In *The Pantanal: Ecology, Biodiversity and Sustainable Management of a Large Neotropical Seasonal Wetland*; Junk, W.J., Wantzen, K.M., da Cunha, C.N., da Silva, C.J., Eds.; Pensoft: Sofia, Bulgaria, 2011; pp. 127–141.
35. Beasley, C.R. The impact of exploitation on freshwater mussel (Bivalvia: Hyriidae) in the Tocantins River Brazil. *Stud. Neotrop. Fauna Environ.* **2001**, *36*, 159–165. [CrossRef]
36. Pimpao, D.M.; Rocha, M.S.; Fettuccia, D.C. Freshwater mussels of Catalão, confluence of Solimões and Negro rivers, state of Amazonas, Brazil. *Check List* **2008**, *4*, 395–400. [CrossRef]
37. Pimpao, D.M.; Mansur, M.C.D. Chave pictórica para identificação dos bivalves do Rio Aripuanã, Amazonas, Brasil (Sphaeriidae, Hyriidae e Mycetopodidae). *Biota Neotrop.* **2009**, *9*, 1–8. [CrossRef]
38. Folmer, O.; Black, M.; Hoeh, W.; Lutz, R.; Vrijnhoek, R. DNA primers for amplification of mitochondrial cytochrome *c* oxidase subunit I from diverse metazoan invertebrates. *Mol. Mar. Biol. Biotechnol.* **1994**, *3*, 294–299.
39. Campbell, D.C.; Serb, J.M.; Buhay, J.E.; Roe, K.J.; Minton, R.L.; Lydeard, C. Phylogeny of North American amblemines (Bivalvia, Unionoida): Prodigious polyphyly proves pervasive across genera. *Invert. Biol.* **2005**, *124*, 131–164. [CrossRef]
40. Walker, J.M.; Curole, J.P.; Wade, D.E.; Chapman, E.G.; Bogan, A.E.; Watters, G.T.; Hoeh, W.R. Taxonomic distribution and phylogenetic utility of gender-associated mitochondrial genomes in the Unionoida (Bivalvia). *Malacologia* **2006**, *48*, 265–282.
41. Varela, E.S.; Beasley, C.R.; Schneider, H.; Sampaio, I.; Marquez-Silva, N.D.S.; Tagliaro, C.H. Molecular phylogeny of mangrove oysters (*Crassostrea*) from Brazil. *J. Molluscan Stud.* **2007**, *73*, 229–234. [CrossRef]

42. Palumbi, S.; Martin, A.; Romano, S.; McMillian, W.O.; Stice, L.; Grabowski, G. *The Simple Fool's Guide to PCR*; Privately published document compiled by S. Palumbi; Department of Zoology, University of Hawaii: Honolulu, HI, USA, 1991.
43. Pleyte, K.A.; Duncan, S.D.; Phillips, R.B. Evolutionary relationships of the salmonid fish genus *Salvelinus* inferred from DNA sequences of the first internal transcribed spacer (ITS 1) of ribosomal DNA. *Mol. Phylogenet. Evol.* **1992**, *1*, 223–230. [CrossRef]
44. Park, J.-K.; O'Foighil, D. Sphaeriid and corbiculid clams represent separate heterodont bivalve radiations into freshwater environments. *Mol. Phylogenet. Evol.* **2000**, *14*, 75–88. [CrossRef] [PubMed]
45. Colgan, D.J.; McLaughlan, A.; Wilson, G.D.F.; Livingston, S.P.; Edgecombe, G.D.; Macaranas, J.; Cassis, G.; Gray, M.R. Histone H3 and U2 snRNA DNA sequences and arthropod molecular evolution. *Aust. J. Zool.* **1998**, *46*, 419–437. [CrossRef]
46. Thompson, J.D.; Higgins, D.G.; Gibson, T.J. Clustal W: Improving the sensitivity of progressive multiple sequence alignment through sequence weighting, position-specific gap penalties and weight matrix choice. *Nucleic Acids Res.* **1994**, *22*, 4673–4680. [CrossRef] [PubMed]
47. Löytynoja, A.; Goldman, N. webPRANK: A phylogeny-aware multiple sequence aligner with interactive alignment browser. *BMC Bioinform.* **2010**, *11*, 579. [CrossRef]
48. Borschenius, F. FastGap 1.2. 2009. Available online: http://www.aubot.dk/FastGap_home.htm (accessed on 4 March 2020).
49. Altschul, S.F.; Gish, W.; Miller, W.; Myers, E.W.; Lipman, D.J. Basic local alignment search tool. *J. Mol. Biol.* **1990**, *215*, 403–410. [CrossRef]
50. Rozas, J.; Librado, P.; Sanchez-Delbarrio, J.C.; Messeguer, X.; Rozas, R. *DnaSP*; Version 5.10.00; Universita de Barcelona: Barcelona, Spain, 2009; Available online: http://www.ub.edu/dnasp/ (accessed on 6 March 2020).
51. Leigh, J.W.; Bryant, D. POPART: Full-feature software for haplotype network construction. *Meth. Ecol. Evol.* **2015**, *6*, 1110–1116. [CrossRef]
52. Clement, M.; Snell, Q.; Walker, P.; Posada, D.; Crandall, K. TCS: Estimating gene genealogies. *Parallel Distrib. Process. Symp. Int.* **2002**, *2*, 0184.
53. Tanabe, A.S. Kakusan4 and Aminosan: Two programs for comparing nonpartitioned, proportional and separate models for combined molecular phylogenetic analyses of multilocus sequence data. *Mol. Ecol. Resour.* **2011**, *11*, 914–921. [CrossRef]
54. Ronquist, F.; Teslenko, M.; Van der Mark, P.; Ayres, D.; Darling, A.; Hohna, S.; Larget, B.; Liu, L.; Suchard, M.A.; Huelsenbeck, J.P. MrBayes 3.2: Efficient Bayesian phylogenetic inference and model choice across a large model space. *Syst. Biol.* **2012**, *61*, 539–542. [CrossRef]
55. Rambaut, A.; Suchard, M.A.; Xie, D.; Drummond, A.J. Tracer 1.6. 2014. Available online: http://beast.bio.ed.ac.k/tracer (accessed on 6 July 2020).
56. Rambaut, A.; Suchard, M.A.; Xie, D.; Drummond, A.J. *MCMC Trace Analysis Tool*; Version 1.6.0; Institute of Evolutionary Biology, University of Edinburgh: Edinburg, Scotland, 2009; Available online: http://tree.bio.ed.ac.uk/software/tracer/ (accessed on 6 July 2020).
57. Puillandre, N.; Lambert, A.; Brouillet, S.; Achaz, G. ABGD, automatic barcode gap discovery for primary species delimitation. *Mol. Ecol.* **2012**, *21*, 1864–1877. [CrossRef]
58. Paradis, E.; Klaus, S.; Schwartz, R. Ape 5.0: An environment for modern phylogenetics and evolutionary analyses in R. *Bioinformatics* **2018**, *1*, 3. [CrossRef] [PubMed]
59. Revell, L.J. Phytools: An R package for phylogenetic comparative biology (and other things). *Meth. Ecol. Evol.* **2012**, *3*, 217–223. [CrossRef]
60. Cornuet, J.M.; Ravigne, V.; Estoup, A. Inference on population history and model checking using DNA sequence and microsatellite data with the software DIYABC (v1.0). *BMC Bioinform.* **2010**, *11*, 401. [CrossRef] [PubMed]
61. Hasegawa, M.; Kishino, H.; Yano, T. Dating the human-ape split by a molecular clock of mitochondrial DNA. *J. Mol. Evol.* **1985**, *22*, 160–174. [CrossRef]
62. Cornuet, J.M.; Santos, F.; Beaumont, M.A.; Robert, C.P.; Marin, J.M.; Baldong, D.J.; Guillemaud, T.; Estoup, A. Inferring population history with DIYABC: A user-friendly approach to approximate Bayesian computation. *Bioinformatics* **2008**, *24*, 2713–2719. [CrossRef]
63. Bonetto, A.A. La Superfamília Unionacea en la cuenca Amazonica. In *Atlas Simpósio Biota Amazônica 3: Limnologia*; Lent, H., Ed.; CNPq: Rio de Janeiro, Brazil, 1967; pp. 63–82.

64. Mansur, M.C.D.; Callil, C.T.; Aguiar, E.P.; Pedroso, L.M.G. *Inventário dos Bivalves Límnicos do rio Cuiabá (MT, Brasil) Como Subsídio para o Reconhecimento da Integridade Ecológica*; Relatório Final; Edital Fundação de Amparo a Pesquisa do Estado de Mato Grosso: Cuiaba, MT, Brazil, 2007.
65. Rodriguez, F.J.L.; Oliver, J.L.; Marin, A.; Medina, J.R. The general stochastic model of nucleotide substitution. *J. Theor. Biol.* **1990**, *142*, 485–501. [CrossRef]
66. Graf, D.L.; Ó Foighil, D. Molecular phylogenetic analysis of 28S rDNA supports a Gondwanan origin for Australasian Hyriidae (Mollusca: Bivalvia: Unionoida). *Vie Milieu* **2000**, *50*, 245–254.
67. Callil, C.T.; Junk, W.J. Concentração e incorporação de mercúrio por moluscos bivalves *Anodotites trapesialis* (Lamarck, 1819) e *Castalia ambigua* (Lamarck, 1819) do Pantanal de Poconé—MT, Brasil. *Biociências* **1999**, *72*, 3–28.
68. Mansur, M.C.D.; Valer, R.M. Moluscos bivalves do Rio Uraricoera e Rio Branco, Roraima, Brasil. *Amazoniana* **1992**, *12*, 85–100.
69. Da Mata, L.S.; Tagliaro, C.H.; Simeone, D.; Robert, C. Shell shape variation in Amazonian freshwater mussels (Unionida: Hyriidae: Hyriini) Beasley. *J. Molluscan Stud.* **2019**, *85*, 212–223. [CrossRef]
70. Haag, W.R. *North American Freshwater Mussels: Natural History, Ecology and Conservation*; Cambridge University Press: Cambridge, UK, 2012.
71. Whelan, N.V.; Geneva, A.J.; Graf, D.L. Molecular phylogenetic analysis of tropical freshwater mussels (Mollusca: Bivalvia: Unionoida) resolves the position of *Coelatura* and supports a monophyletic Unionidae. *Mol. Phylogenet. Evol.* **2011**, *61*, 504–514. [CrossRef] [PubMed]
72. Zieritz, A.; Hoffman, J.I.; Amos, W.; Aldridge, D.C. Phenotypic plasticity and genetic isolation-by-distance in the freshwater mussel *Unio pictorum*. *Evol. Ecol.* **2010**, *24*, 923–938. [CrossRef]
73. Bolotov, I.N.; Makhrov, A.A.; Gofarov, M.Y.; Aksenova, O.V.; Aspholm, P.E.; Bespalaya, Y.V.; Kabakov, M.B.; Kolosova, Y.S.; Kondakov, A.V.; Ofenböck, T.; et al. Climate warming as a possible trigger of keystone mussel population decline in oligotrophic rivers at the continental scale. *Sci. Rep.* **2018**, *8*, 35. [CrossRef] [PubMed]
74. Inoue, K.; Hayes, D.M.; Harris, J.L.; Christian, A.D. Phylogenetic and morphometric analyses reveal ecophenotypic plasticity in freshwater mussels *Obovaria jacksoniana* and *Villosa arkansasensis* (Bivalvia: Unionidae). *Ecol. Evol.* **2013**, *3*, 2670–2683. [CrossRef] [PubMed]
75. Prie, V.; Puillandre, N. Molecular phylogeny, taxonomy, and distribution of French *Unio* species. *Hydrobiologia* **2014**, *735*, 95–110. [CrossRef]
76. Lundberg, J.G.; Marshall, L.G.; Guerrero, B.H.; Malabarba, M.C.S.L.; Wesselingh, F. The stage for Neotropical fish diversification: A history of tropical South American rivers. In *Phylogeny and Classification of Neotropical Fishes*; Malabarba, L.R., Reis, R.E., Vari, R.P., Lucena, Z.M., Lucena, C.A.S., Eds.; Edipucrs: Porto Alegre, Brazil, 1998; pp. 13–48.